Stem Cell Reports
Resource
ISSCR
OPEN ACCESS

Molecular Profiling Reveals Involvement of ESCO2 in Intermediate Progenitor Cell Maintenance in the Developing Mouse Cortex

Pauline Antonie Ulmke,[1,6] M. Sadman Sakib,[2,6] Peter Ditte,[3,6] Godwin Sokpor,[1,5,6] Cemil Kerimoglu,[2] Linh Pham,[1,5] Yuanbin Xie,[1] Xiaoyi Mao,[1] Joachim Rosenbusch,[1] Ulrike Teichmann,[3] Huu Phuc Nguyen,[5] Andre Fischer,[2,4] Gregor Eichele,[3] Jochen F. Staiger,[1] and Tran Tuoc[1,5,*]

[1]Institute for Neuroanatomy, University Medical Center, Georg-August-University, Goettingen, Germany
[2]German Center for Neurodegenerative Diseases, Goettingen, Germany
[3]Max-Planck-Institute for Biophysical Chemistry, Goettingen, Germany
[4]Cluster of Excellence "Multiscale Bioimaging: from Molecular Machines to Networks of Excitable Cells" (MBExC), Goettingen, Germany
[5]Department of Human Genetics, Ruhr University of Bochum, Bochum, Germany
[6]These authors contributed equally
*Correspondence: tran.tuoc@ruhr-uni-bochum.de
https://doi.org/10.1016/j.stemcr.2021.03.008

SUMMARY

Intermediate progenitor cells (IPCs) are neocortical neuronal precursors. Although IPCs play crucial roles in corticogenesis, their molecular features remain largely unknown. In this study, we aimed to characterize the molecular profile of IPCs. We isolated TBR2-positive (+) IPCs and TBR2-negative (−) cell populations in the developing mouse cortex. Comparative genome-wide gene expression analysis of $TBR2^+$ IPCs versus $TBR2^-$ cells revealed differences in key factors involved in chromatid segregation, cell-cycle regulation, transcriptional regulation, and cell signaling. Notably, mutation of many IPC genes in human has led to intellectual disability and caused a wide range of cortical malformations, including microcephaly and agenesis of corpus callosum. Loss-of-function experiments in cortex-specific mutants of *Esco2*, one of the novel IPC genes, demonstrate its critical role in IPC maintenance, and substantiate the identification of a central genetic determinant of IPC biogenesis. Our data provide novel molecular characteristics of IPCs in the developing mouse cortex.

INTRODUCTION

In developing cerebral cortex, intermediate progenitor cells (IPCs) are transit-amplifying cells that express the T-box transcription factor (TF) TBR2 (Hevner, 2019). IPCs are basal derivatives of the multipotent radial glial progenitor cells (RGCs) in developing cortex, and they exclusively differentiate into glutamatergic neurons. Although IPCs are known to give rise to the majority of cortical neurons (Haubensak et al., 2004; Kowalczyk et al., 2009; Miyata et al., 2004; Noctor et al., 2004), the molecular factors that drive or maintain the transient proliferative capacity and neurogenic properties of TBR2-positive ($TBR2^+$) IPCs in the subventricular zone (SVZ) niche remain incompletely explored. The identification of the gene expression program that governs the genesis and maintenance of IPCs would improve our understanding of cortical development and provide possible protocols to culture IPCs *in vitro* or generate these cortical progenitors by cell reprogramming from other cell sources. Moreover, a description of the molecular features of IPCs can provide insights into the genes implicated in the etiology of pertinent neurological disturbances caused by defective IPC genesis.

To understand the molecular signatures of cell types in developing cortex, researchers have employed single-cell RNA sequencing (scRNA-seq) analyses to provide the molecular identity of cell subtypes, including IPCs in mouse (Kawaguchi et al., 2008; Li et al., 2020; Loo et al., 2019; Telley et al., 2016) and human cortex (Fan et al., 2018; Li et al., 2018; Nowakowski et al., 2017; Pollen et al., 2015; Zhong et al., 2018). However, due to the threshold of high-throughput scRNA-seq, profiling cell-type-specific gene expression is challenging. Comparisons between transcriptome analyses from purified cell populations have contributed additionally insightful molecular information about cortical cell subtypes (Albert et al., 2017; Amamoto et al., 2020; Arlotta et al., 2005; Molyneaux et al., 2015; Pinto et al., 2008).

In the present study, we used an antibody to label intranuclear TBR2 in single-nuclei suspensions isolated from embryonic day 16.5 (E16.5) mouse cortex and then sorted the $TBR2^+$ cells (taken as IPCs) from the $TBR2^-$ cells (taken as non-IPCs). We then identified the expression of IPC-enriched genes by RNA-seq. Using high-throughput *in situ* hybridization (ISH) (Visel et al., 2004), we confirmed the so far SVZ-restricted expression of 392 novel IPC genes. The *in situ* expression of these genes is freely available online in an interactive database (https://gp3.mpg.de). A comparison of mouse IPC transcriptome and human phenotype annotations suggests that these IPC-enriched genes play important roles in cortical development in humans, as such patients with mutation variants display a wide range of cortical malformation and intellectual disability. Comparative genome-wide gene expression analysis of $TBR2^+$ IPCs versus $TBR2^-$ cells revealed changes in key factors for chromatid segregation, cell-cycle

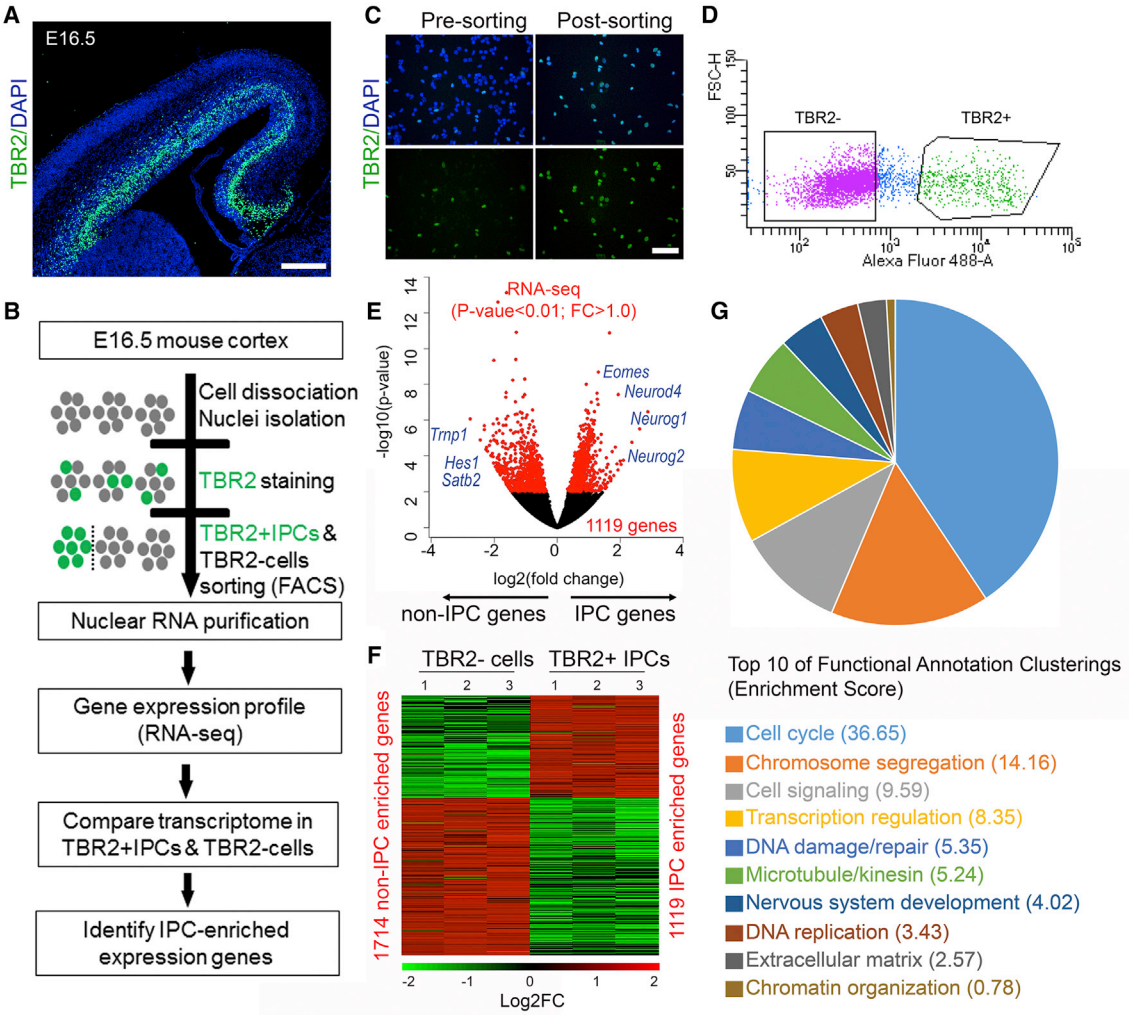

(legend on next page)

regulation, transcription regulation, and chromatin remodeling. Among them, establishment of sister chromatid cohesion *N*-acetyltransferase 2 (ESCO2) was selected for confirmative studies. The cortex-specific mutagenesis for *Esco2* caused a massive depletion of the IPC population, thus validating that we identified a central genetic determinant of IPC maintenance.

RESULTS

Sorting and Transcriptome Profiling of Intermediate Progenitor Cells in Developing Mouse Cortex

To compare the transcriptome profile of TBR2$^+$ IPCs and TBR2$^-$ cells in mouse developing cortex (Figure 1A), we isolated nuclei and established an intranuclear immunofluorescent staining and fluorescence-activated cell sorting (FACS) protocol (Figure 1B). We used intranuclear TBR2 antibody labeling in single-nuclei suspensions isolated from E16.5 mouse cortices followed by cell sorting (Figure 1C) (Sakib et al., 2021). Sorting gates were adjusted to purify TBR2$^+$ IPC and TBR2-cell nuclei. Unlike unsorted nuclei suspensions, sorted nuclei suspensions were highly enriched (i.e., >99%) in the desired cell type (Figures 1C and 1D).

To understand the gene-regulatory difference in these cell populations, we generated RNA-seq libraries with three biological replicates for each cell populations. As anticipated, a high expression of canonical IPC genes was observed in the IPC population consistent with known *in vivo* expression patterns (Figures 1E, 1F, and S1A–S1C; Table S1). Comparing the expression of housekeeping genes, which locate on chromosome X (*Xist*, *Pgk1*, *Hprt*, *Eif2s3x*) and chromosome Y (*Ddx3y*, *Eif2s3y*), revealed their comparable expression level in samples from TBR2$^+$ IPCs and TBR2$^-$ cells (Figure S1C). The data suggest that TBR2$^+$ and TBR2$^-$ cell populations were derived from a similar number of female and male embryos.

Next, we sought to identify genes with significant differences in expression level between the two cell populations and used these expression estimates to identify clusters. Cuffdiff2 was used to identify 1,119 enriched IPC genes (1,050 protein-coding RNAs and 69 long non-coding RNAs [lncRNAs]) and 1,714 enriched non-IPC genes with significant differential expression between the cell types ($p < 0.01$ and |fold change| (FC) > 1.0, Figures 1E and 1F). The IPC-enriched genes were annotated into different functional categories (Figures 1G, S1D, and S1E; Table S2; see experimental procedures). The significance of such predominating gene clusters was analyzed and is discussed later.

The reliability of our analyses was ensured by validating the expression pattern of the identified IPC-enriched genes in developing mouse cortex. ISH for 392 of such genes confirmed their restricted expression in SVZ in the E14.5 cortex, which is consistent with their RNA expression profiles (Table S3). To further validate the quality of our RNA-seq data, we performed immunohistochemical analysis of the E15.5 mouse cortex for ESCO2 as one of novel IPC factors. ESCO2 protein expression was mainly observed in the germinative zone of the developing cortex, especially the basal aspect (Figure 1H). Quantification revealed that most of the cells expressing ESCO2 also expressed the IPC marker TBR2, but to a lesser extent in cells in the transition stage between RGC-IPC (PAX6$^+$/TBR2$^+$) and in RGCs (PAX6$^+$) (Figure 1I).

Previous studies, which have characterized the transcription profiles of single cells isolated from the developing mouse cortex, have generated a repository of genes enriched in each of the murine cortical cell types (Kawaguchi et al., 2008; Li et al., 2020; Loo et al., 2019; Telley et al., 2016). To identify novel IPC genes that might play essential roles in the development of this cell type, we compared the list of mouse IPC genes from those scRNA-seq experiments and from sorted TBR2$^+$ IPCs (this study) and found that our list of IPC-enriched genes contains most of the previously

Figure 1. Cell Sorting and Gene Expression Profiling of Mouse TBR2$^+$ IPCs

(A) Micrograph showing the E16.5 mouse cortex immunostained with TBR2 antibody. Counterstaining was done with 4′,6-diamidino-2-phenylindole (DAPI).

(B) An illustration of the experimental design used to sort out TBR2-labled IPCs and subsequent nuclear analysis to compare the transcriptional profile of IPCs in mouse.

(C) Representative images of pre- and post-sorted cell suspensions from mouse cortex stained with TBR2 antibody. Counterstaining was done with DAPI.

(D) Representative plot showing sorting gates for TBR2$^+$ and TBR2$^-$ cells from mouse and human cortex.

(E and F) Volcano plot (E) and heatmap (F) showing the enrichment of IPC and non-IPC genes in corresponding sorted cell populations.

(G) Pie chart showing proportions of the enrichment score of the top ten functional annotation clustering in IPCs.

(H) Micrograph of immunohistochemical (IHC) staining showing the E15.5 wild-type mouse cortex at low and high magnification stained with ESCO2, TBR2, and PAX6 antibodies. Cortical area with high magnification is indicated by a white box. Arrows point to TBR2$^+$ IPCs co-expressing ESCO2 but not PAX6.

(I) Composite bar graph showing the quantitative proportion of ESCO2$^+$ cells co-expressing PAX6 or TBR2 or both in germinal zone of the E15.5 mouse cortex. n = 6 experimental replicates.

Scale bars, 100 μm (A) and 50 μm (C and H).

identified IPC genes (Figure S1E). Intriguingly, 961 out of the 1,121 IPC-enriched genes from this study (Figure S1D) were not present in any of the gene lists of the aforementioned studies. Gene ontology (GO) analysis indicated that these novel IPCs encode for proteins belonging to different families of factors, such as chromatin/epigenetic factors, DNA- and RNA-binding factors, and post-transcription/-translation modification factors (Table S2 and Figure S1E).

Together, these results demonstrate an efficient isolation of mouse TBR2$^+$ IPCs, which allow adequate molecular profiling.

Predominance of Mitotic Cell-Cycle-Related and Mitotic Chromatid-Segregation-Related Gene Signatures in IPCs

Previous studies revealed that IPCs are transient cortical progenitors that actively undergo mitotic cell divisions (Hevner, 2019). Consistent with these features of IPCs, many of the genes in the top GO pathways belong to cell-cycle- and cell-division-related categories (Figure 2A). Remarkably, our gene expression profiling revealed that genes encoding for many cyclin and cyclin cofactors are highly expressed in IPCs (Figures 2B and 2C; Table S4). Examination of these cell-cycle-regulation genes in subtypes of IPCs might offer a yardstick for distinguishing neurogenic IPCs from proliferative IPCs.

During cell division, chromosomes need to be segregated and evenly distributed among daughter cells to ensure accurate passing of genetic information to the next generation. In addition to the alterations in mRNA levels for genes involved in cell-cycle regulation, high expression of genes related to DNA replication, repair, and chromatid segregation were observed (Figure 2A and Table S4). Particularly, expression of genes encoding for subunits of the chromosome segregation machinery is highly enriched in IPCs, e.g., Cohesin complex (*Sgol1*, *Sgol2*, *Smc3*, *Rec8*, *Cdca5*, and *Wapal*), Condensin complex (*Ncapd2*, *Ncapd3*, *Ncapg*, *Ncaph*, *Smc2*, and *Smc4*), Minichromosome maintenance complex (*Mcm2*, *Mcm3*, *Mcm4*, *Mcm5*, *Mcm6*, *Mcm7*, and *Mms22l*), and Smc5-Smc6 complex (*Smc5*, *Smc6*, *Nsmce2*, and *Nsmce4a*) (Figures 2D and 2E; Table S4). Single gene factors (e.g., *Esco2*, *Spag5*, *Ncapg*) involved in chromosome segregation were also identified in IPCs (Figure 2D and 2E).

The results shown here indicate that the expression of many cell-cycle and chromatid-segregation genes is associated with, and supportive for, the highly active cell division of IPCs.

Many IPC-Enriched Genes Belong to Signaling Pathways

Pathway enrichment analysis revealed that several brain-regulating signaling pathways are significantly enriched in IPC genes, including the p53-Caspase cascade, Hippo, Notch, FoxO, PI3K-Akt, Axon guidance, and Fanconi anemia signaling pathway (Figure 3A). Corroborating the results from the transcriptomics analysis, we confirmed an enrichment of several genes belonging to these signaling pathways in the SVZ (Figures 3B–3Q). The identified signaling pathways may play unique roles in the proliferation, differentiation, and/or survival of IPCs during cortical development.

Cell lineage tracing experiments with TBR2-CreER indicated that the majority of IPC derived clones (~66%) generate one daughter cell as neuron and another as apoptotic cell, indicating asymmetric cell death (Mihalas and Hevner, 2018). The observed remarkable abundance of apoptosis of IPC daughter cells is in accordance with previous findings of a high level of cell death in the SVZ (Blaschke et al., 1996; Thomaidou et al., 1997). These outcomes are congruent with our GO analysis, which revealed that many genes belonging to the p53 signaling cascade and caspase signaling pathway, which lead to apoptosis, are enriched in IPCs (Figures 3B–3E and Table S5). Indeed, immunohistochemical analysis indicated a large proportion of CASP3$^+$ cells immunoreactive with TBR2 in the developing mouse cortex at E16.5 (Figure S2), corroborating the finding that more than half the progenies of IPCs undergo apoptotic cell death in the normally developing cortex (Mihalas and Hevner, 2018).

Hippo signaling is necessary for determination of cell fate and organ size (Zheng and Pan, 2019). Emerging evidence shows the involvement of the Hippo signaling alone or cooperatively with other signaling pathways in brain development (Ouyang et al., 2020). As shown in our transcriptomic analysis, genes involved in the Hippo signaling pathway are prominently expressed in IPCs (Figures 3F and 3G) and likely are critical for the regulation of cortical size via control of IPC genesis (Kostic et al., 2019). Other signaling pathways such as the Delta-Notch (Figures 3H and 3I), FoxO (Figures 3J and 3K), PI3K-Akt (Figures 3L and 3M), Axon guidance (Figures 3N and 3O), and Fanconi anemia (Figures 3P and 3Q) were also identified to be enriched in IPCs. These signaling pathways may play critical roles in the normal progression of brain morphogenesis via modulation of IPC biogenesis.

Together, the enrichment of signaling pathway genes in the sorted IPCs is indicative of their necessity in sustaining the neuronal progenitor properties of IPCs in the SVZ niche and to permit their function in cortical morphogenesis.

Identification of New IPC-Specific Transcription and Epigenetic Regulators

Many of the genes identified in IPCs were found to participate in the regulation of transcription, chromatin remodeling, and other epigenetic processes (Figure 4A). We first

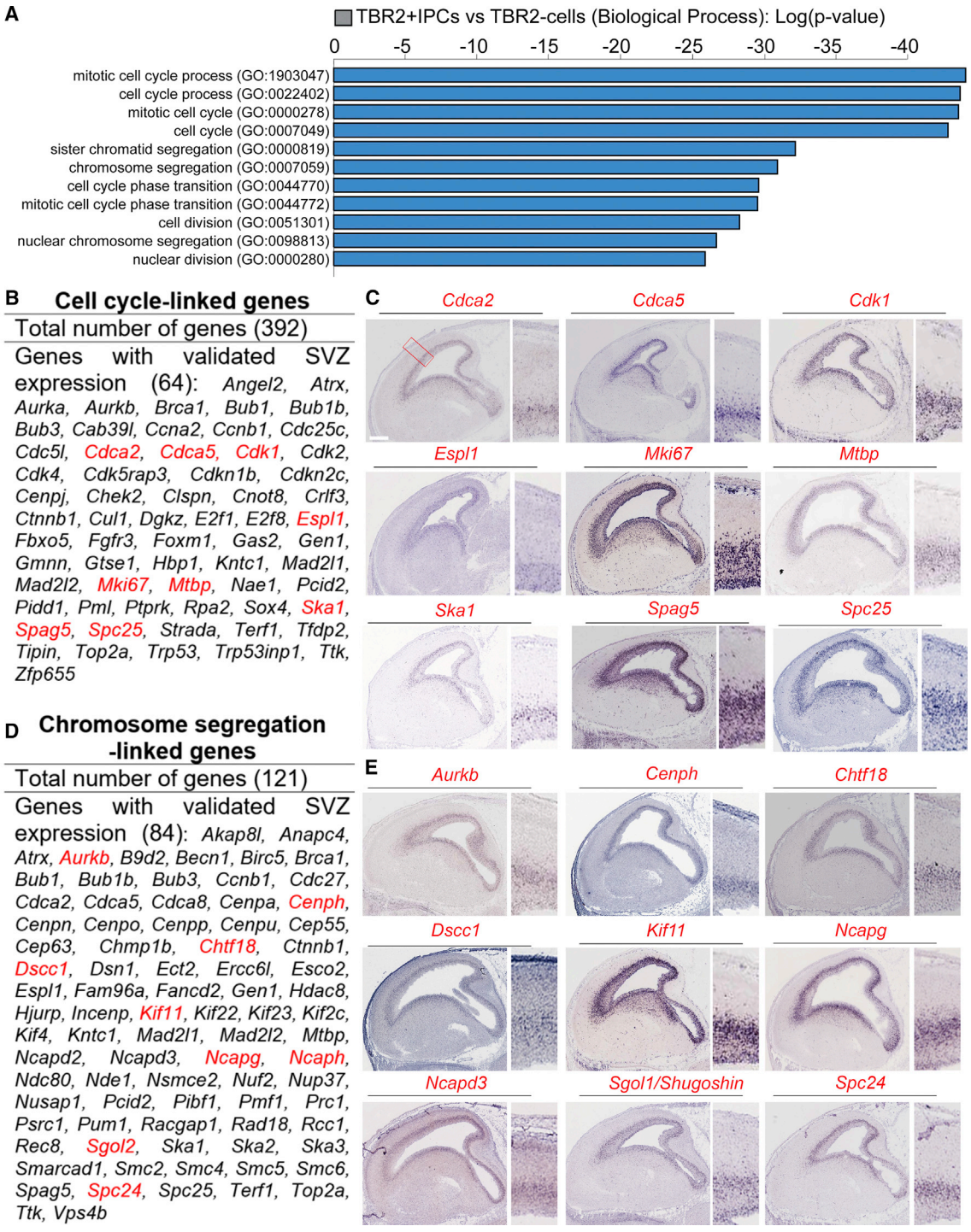

Figure 2. Expression of Many Cell-Cycle and Chromatid-Segregation Genes Are Enriched in IPCs

(A) Graphical representation of gene ontology analysis with terms related to cell cycle and segregation of chromatids.

(B and D) List of the genes identified in IPCs that functionally fall under cell-cycle- and chromosome-segregation-related processes, respectively.

(C and E) Respective array of micrographs showing *in situ* hybridization of examples of the identified genes (highlighted red in B and D) with distinctive expression in the developing mouse cortical subventricular zone, and related to cell-cycle and chromosome-segregation events. Magnified cortical region is shown by a red box in (C). Scale bar, 100 μm.

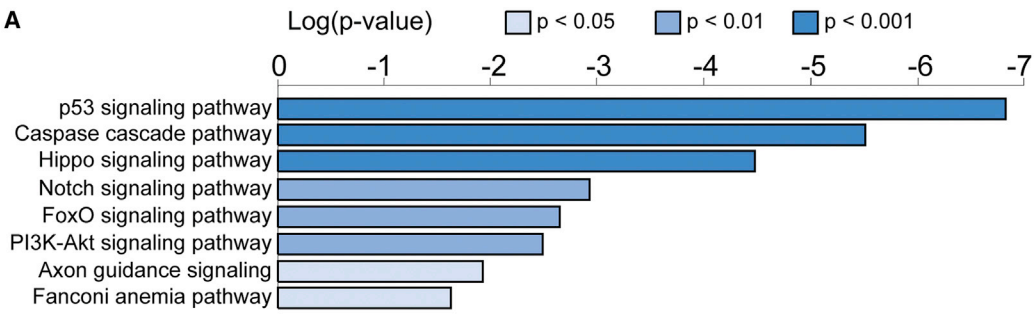

B **p53 signaling-linked genes**
Total number of genes (16): *Ccnb1, Ccnb2, Ccnd2, Ccne1, Ccne2, Cdk2, Cdk6, Chek2, Gadd45a, Gadd45g, Gtse1, Perp, Pidd1, Rrm2, Sesn1, Sesn2*

D **Caspase cascade-linked genes**
Total number of genes (14): *Casp2, Casp6, Casp8ap2, Cfl2, Cradd, Diablo, Gas2, Numa1, Pidd1, Ripk1, Srebf1, Top1, Traf2, Trp53*

F **Hippo signaling-linked genes**
Total number of genes (20): *Amot, Birc5, Ccnd2, Ctnna1, Fzd2, Fzd3, Fzd6, Gli2, Lef1, Limd1, Mpp5, Stk3, Tcf7l2, Tead1, Tead2, Tead3, Tgfb2, Tgfbr2, Wnt10a, Wnt5a*

H **Notch signaling-linked genes**
Total number of genes (9): *Dll1, Dll3, Dll4, Hdac1, Maml3, Mfng, Ncstn, Notch1, Numb*

J **FoxO signaling-linked genes**
Total number of genes (15): *Bcl2l11, Ccnb1, Ccnb2, Ccnd2, Cdk2, Foxo3, Gadd45a, Gadd45g, Irs1, Pck2, Pik3r3, Slc2a4, Stat3, Tgfb2, Tgfbr2*

L **PI3K-Akt signaling genes**
Total number of genes (28): *Bcl2l11, Brca1, Ccnd2, Ccne1, Ccne2, Cdk2, Cdk6, Col4a5, Col5a1, Col5a2, Creb3l2, Creb5, Ddit4, F2r, Foxo3, Irs1, Itga4, Itga7, Itga9, Itgb1, Lama2, Lama5, Lamb2, Lpar1, Lpar4, Lpar6, Pck2, Pik3r3*

N **Axon guidance-linked genes**
Total number of genes (13): *Cxcl12, Dcc, Epha3, Epha4, Ephb4, Itgb1, Nfatc4, Ntng2, Pak4, Sema3c, Sema3g, Sema5a, Unc5d*

P **Fanconi anemia-linked genes**
Total number of genes (7): *Brca1, Brip1, Eme1, Fancd2, Fanci, Rad51, Ube2t*

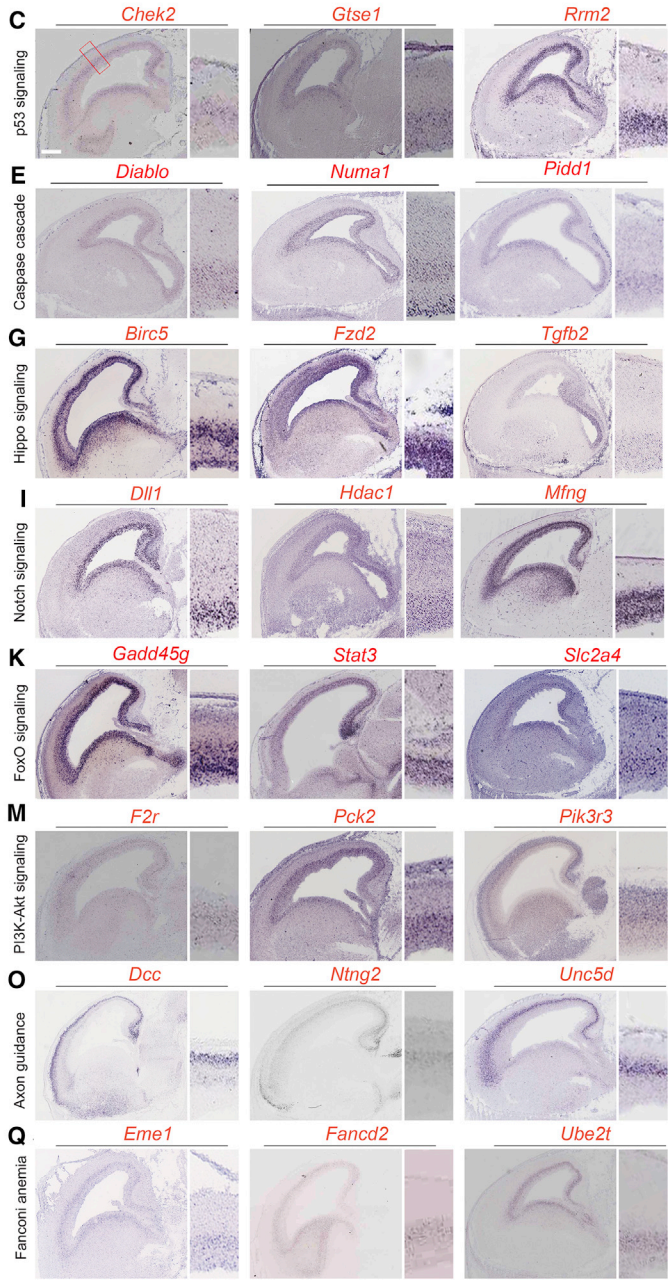

(legend on next page)

looked for epigenetic and chromatin regulators, which are highly expressed in IPCs. We found enrichment of epigenetic genes in the sorted IPCs: a total of 66 genes, 25 of which were validated by ISH (Figures 4B and 4C; Table S6). Such epigenetic genes include Deacetylase genes, genes related to the PRC2 complex, and genes encoding for Methyltransferase domain-containing proteins.

A set of IPC genes which encode for protein factors that form complexes to regulate chromatin dynamics was identified. In all we found 52 such genes markedly expressed in IPCs, and with distinctive expression in the SVZ for at least 24 of them (Figures 4D and 4E; Table S6). The identified chromatin-modification-related genes belong to the following classes of chromatin remodelers: SWI/SNF superfamily-type complex, ISWI-type complex, and NuRD/CHD complex (Table S6).

Besides epigenetic and chromatin regulators, our data provided a context to examine the relative contribution of specific non-coding RNAs (ncRNAs) and TFs to IPC identity and/or regulation. We identified 69 known lncRNA and three small nucleolar RNA genes, with significantly higher level of expression in TBR2$^+$ IPCs compared with TBR2$^-$ cells ($\log_2$FC > 1.0, $p < 0.01$) (Figures 4F and 4G; Table S6). Among these ncRNAs, ISH analysis confirmed the restricted expression of three lncRNAs (*A930024E05Rik*, *5330426P16Rik*, and *9630028B13Rik*, Figure 4G) in SVZ of the developing cortex.

We identified 104 IPC genes encoding TFs belonging to more than four protein families (Figures 4H, 4I, and S3; Table S6). C2H2-type zinc finger protein family was the most enriched protein family, with 47 upregulated genes, followed by basic-helix-loop-helix/Myb and homeobox protein families, with nine upregulated genes each. The LIM TF family genes were also found in the purified IPCs (Figures S3A–S3I). The genes encoding for TFs, which were found to exhibit a high expression in IPCs, included many known key regulators of neurogenesis such as *Eomes* (*Tbr2*), *Ngn1*, *Ngn2*, *NeuroD1*, and *Bag2*, as well as many as yet uncharacterized genes (e.g., *Nhlh1*, *Csrp1*, and *Mybl2*; Figure 4H) that may prove to be novel regulators of cortical development.

Next, we determined which of the TFs interact physically or functionally using the STRING database. This revealed a highly interconnected network formed by IPC-enriched TFs. Several TFs formed a network hub. Among them CBFA2T2, NEUROG2, NEUROG1, STAT3, NEUROD1, and TCF3 appear to be in the center of the network, as they interact with many other TFs (Figure 4J). This raises the possibility that the components of this TF network are key determinants in IPC biogenesis.

Taken together, our findings indicate that major elements of the transcriptional and epigenetic machinery are distinctively present in mouse IPCs.

Gene Expression Profiling Suggests Mutations of IPC-Enriched Genes Have Implications for Cortical Neurodevelopmental Disorders in Human

Recent single-cell transcriptomic analysis of the human developing cortex identified a large set of IPC genes (Fan et al., 2018; Li et al., 2018; Nowakowski et al., 2017; Pollen et al., 2015; Zhong et al., 2018) and IPC lncRNAs (Liu et al., 2016). To further study the developmental and evolutionary origin of the transcriptional signature of IPC cells, we compared these published scRNA data for human developing cortex with those for mouse developing cortex (Kawaguchi et al., 2008; Li et al., 2020; Loo et al., 2019; Telley et al., 2016) and with bulk RNA-seq for mouse TBR2$^+$ IPCs (this study, Figure S4). The comparisons revealed not only a remarkable match between the two species but also highlighted an expanded gene expression program in human IPCs (Figure S4).

Mutations of the IPC-specific gene *TBR2* cause microcephaly and a wide range of cortical anomalies in both rodent (Arnold et al., 2008; Mihalas et al., 2016; Sessa et al., 2008) and human (Baala et al., 2007). In addition to congenital microcephaly, the affected individuals presented with dilatation of cerebral ventricles, agenesis of corpus callosum, polymicrogyria, and dysgenic cerebellum (Baala et al., 2007). The affected children also exhibited severe motor deficits, with hypotonia and intellectual disability (Baala et al., 2007).

To identify a potential involvement of these common IPC genes (Figure S4B), which were found both in developing cortices from mouse (this study) and human (Fan et al., 2018; Li et al., 2018; Nowakowski et al., 2017; Pollen et al., 2015; Zhong et al., 2018), in human diseases, we performed systematic human phenotype ontology analysis (Robinson et al., 2008) (Figure 5A). Mutations of many

Figure 3. IPC-Enriched Genes Encode for Variety of Signaling Pathway Factors

(A) Graphical representation of the top-ranked signaling pathways that are prominent in IPCs.

(B, D, F, H, J, L, N, and P) List of the genes identified in IPCs that are involved in the p53, Caspase, Hippo, Notch, FoxO, PI3K-Akt, Axon guidance, and Fanconi anemia signaling pathways, respectively.

(C, E, G, I, K, M, O, and Q) Respective array of micrographs showing *in situ* hybridization of examples of the identified signaling pathway-linked genes (highlighted red in the adjoining gene list) with distinctive expression in the developing mouse cortical subventricular zone. Magnified cortical region is shown by a red box in (C). Scale bar, 100 μm.

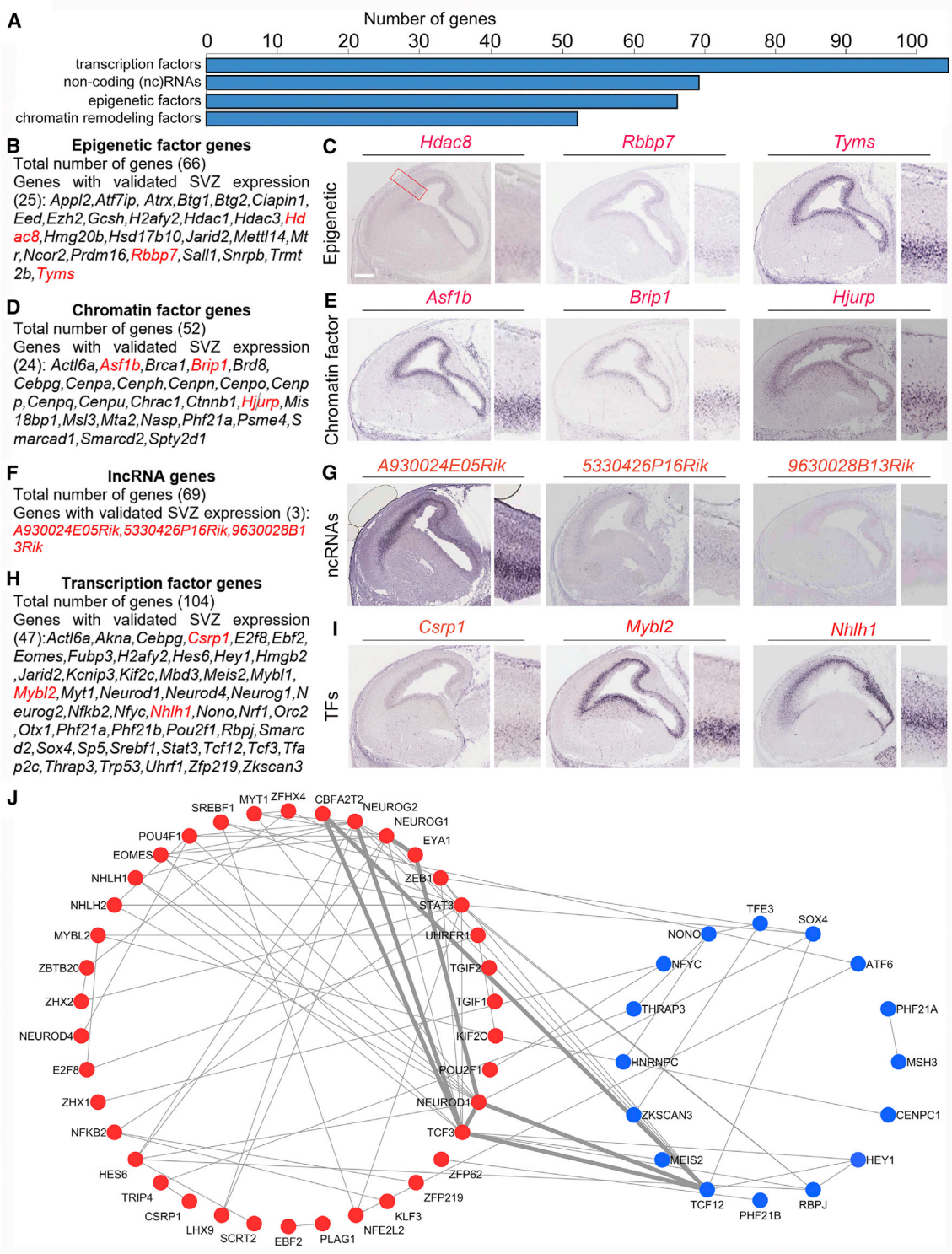

Figure 4. Identification of Novel IPC-Specific Transcription Regulators

(A) Graphical representation of the total number of newly identified genes and their categorization in IPCs that have the potential to regulate transcription.

(B, D, F, and H) List of the genes identified in IPCs that are transcription regulators and can be grouped as epigenetic, chromatin, lncRNA, and transcription factors, respectively.

(legend continued on next page)

IPC genes were found to be associated with intellectual disability phenotype, thus supporting the idea that the perturbation of many biological pathways in IPCs can undermine cognitive development. To determine possible convergence of the various molecular pathways on intermediate phenotypes within the scope of intellectual disability, including brain structure malformations, we looked for correlated phenotypes among the 134 intellectual disability genes (Figures 5B and 5C; Table S7). We identified two major associated phenotypes: (1) microcephaly and (2) corpus callosum agenesis (Figures 5D–5G and Table S7). This observation supports the findings that IPCs generate most of the cortical projection neurons, especially upper layer/callosal neurons, which are necessary for appropriate cortical size and proper establishment of cortical neuron connections across the corpus callosum.

In summary, many gene sets encode for components of the transcriptional, chromatin, and signaling machineries in mouse IPCs, with known or putative regulatory function in cell division, proliferation, differentiation, and survival (Figure 5H). Our data support the possibility that key elements in the mouse IPC transcriptome may be conserved in human and play important roles in cortical development, and their mutations plausibly underlie cortical malformations and dysfunction in both species.

Uncovering ESCO2 as a Novel IPC-Enriched Gene Essential for SVZ Formation and Cortical Neurogenesis

Among the novel IPC genes, *Esco2* is in the top 100 IPC most-enriched genes (Table S1). GO analysis also revealed that *Esco2* belongs to the top gene categories, including cell cycles, chromatin segregation, transcription regulation, DNA replication, and chromatin organization pathways (Tables S2, S4, S5, S6, and S7). Mechanistically, *Esco2* and its ortholog *Esco1*, encoding for cohesin acetyltransferases, are essential for establishing cohesion between sister chromatids by acetylating the SMC3 subunit of the cohesion ring (Nishiyama et al., 2010; Rolef Ben-Shahar et al., 2008; Unal et al., 2008). In contrast to a highly enriched expression of *Esco1* in RGCs in the ventricular zone (VZ) (Figures S5A–S5C), expression of *Esco2* is mostly restricted to IPCs in the SVZ (Figures 1H and 1I; Figures S5D–S5F). This raises a possibility that ESCO1 and ESCO2 play an important role in biogenesis of RGCs and IPCs, respectively.

To understand the role of selected IPC-specific genes in corticogenesis, we characterized functions of *Esco2* in IPC development. Previously it was shown that *Esco2* has a critical role in the formation of cortical layers (Whelan et al., 2012b), and its *de novo* mutations cause primary microcephaly in patients with Roberts syndrome (Vega et al., 2005), suggesting that it might have vital, yet undiscovered, roles in the specification and viability of IPCs and in orchestrating cortical neurogenesis.

To find out the functional significance of ESCO2 during cortical development, we ablated *Esco2* gene in the early developing mouse cortex using an Emx-Cre driver (Gorski et al., 2002; Whelan et al., 2012b). Similar to the gradient expression pattern of Emx1, Emx1-Cre activity is found first in the medial-dorsal cortex (MCX and DCX) at E10.5 and extends to the lateral cortex (LCX) from E12.5 onward (Gorski et al., 2002). Because the Emx1-Cre activity differs in different cortical areas, we first examined the cortical phenotype of *Esco2*cKO (conditional knockout) mutants in MCX and DCX areas (Figure 6A). At E12.5, the ESCO2-ablated cortex displayed a notable reduction in thickness or size compared with control (Figure 6A). A closer examination revealed a reduction in the population of $PAX6^+$ RGCs in the *Esco2*cKO cortex compared with controls (Figures 6A and 6B). Strikingly, the pool of the $TBR2^+$ IPCs is largely lost in MCX and DCX areas of mutants (Figures 6A and 6B). As indicated by immunostaining for the apoptotic cell marker CASP3, there was overt cell death in the E12.5 *Esco2*cKO mutant cortex in the examined cortical areas (Figure 6C).

In accordance with the Emx1-Cre activity, the cortical phenotype of *Esco2*cKO mutants appeared milder in LCX than in MCX and DCX (Figures 6A–6C). Particularly, the population of $PAX6^+$ RGCs and $TBR2^+$ IPCs were reasonably preserved in the cKO LCX (Figures 6A and 6B). In addition, the $CASP3^+$ apoptotic cells were found mostly in the basal side of mutant LCX (Figure 6C). Of note, further differential analysis indicated that majority of the cells undergoing apoptosis in the *Esco2*cKO LCX were $TBR2^+$ IPCs (Figures 6C–6E, empty arrows) and cells in transition stage between RGCs and IPCs (i.e., $PAX6^+$ and $TBR2^+$) (Figures 6C–6E, filled arrows), albeit other cortical cell types such as $PAX6^+$ RGCs and $NEUN^+$ post-mitotic neurons also registered apoptotic activity but to a lesser extent (Figures 6D and 6E).

(C, E, G, and I) Respective array of micrographs showing *in situ* hybridization of examples of the identified transcription regulation genes (highlighted red in the adjoining gene list) with distinctive expression in the developing mouse cortical subventricular zone. Magnified cortical region is shown by a red box in (C). Scale bar, 100 μm.

(J) Protein-protein interaction network of the IPC-enriched transcription factors (TFs). The list of TFs were imported into the STRING database (http://string-db.org/), and the physical or functional interactions between the differentially expressed transcription factors were extracted using the default settings. The red and blue nodes represent IPC-enriched TFs with $\log_2FC > 1.0$ and $0.3 < \log_2FC < 1.0$, respectively. The thin lines indicate low interaction score (<0.4) while the thick lines indicate medium or high interaction score (≥ 0.4).

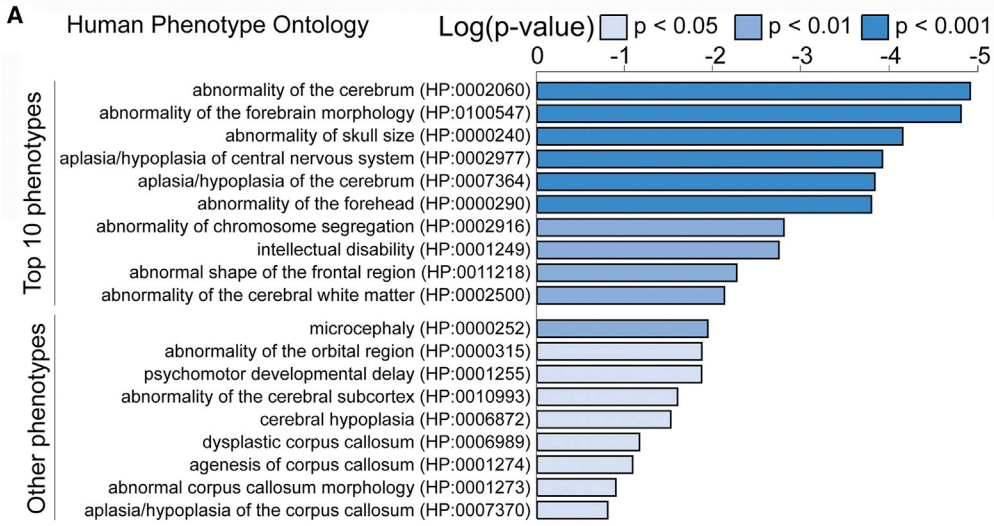

B **Intellectual disability-linked genes**

Total number of genes (134)

Genes with validated SVZ expression (48): *ADSL, AGA, AIFM1, ALDH3A2, ALDH7A1, ATP7A, ATRX, BCAP31, BRIP1, CCDC88C, CDT1, CENPJ, CEP135, CEP63, CKAP2L, CRKL, CTNNB1, CXCL12, CWC27, DCC, DPYD, EED, ESCO2, EZH2, FGFR3, GTF2E2, HDAC8, HSD17B10, IER3IP1, IKBKG, KIF11, KIF4A, LARP7, MEIS2, NDE1, NONO, PHF21A, PHF6, PSAT1, RAD51, RBPJ, SLC16A2, SLC2A1, SNAP29, SNRPB, ST3GAL5, STRADA, TACO1, TCF12, TINF2, VRK1, UBE2T, ZBTB18*

D **Microcephaly-linked genes**

Total number of genes (77)

Genes with validated SVZ expression (33): *ADSL, AGA, ATP7A, ATRX, BCAP31, BRCA1, BUB1B, CDT1, CENPJ, CEP135, CEP63, CKAP2L, CTNNB1, DPYD, ESCO2, HDAC8, IER3IP1, IKBKG, KIF11, LARP7, MCM4, MGME1, NDE1, NEUROG1, PEX19, PHF6, PSAT1, RAD51, SASS6, SLC16A2, SLC2A1, SNAP29, SNRPB, VRK1, ST3GAL5, ZBTB18*

F **Corpus callosum Agenesis-linked genes**

Total number of genes (26)

Genes with validated SVZ expression (7): *DCC, DPYD, FGFR3, NDE1, SASS6, SEMA3C, ZBTB18*

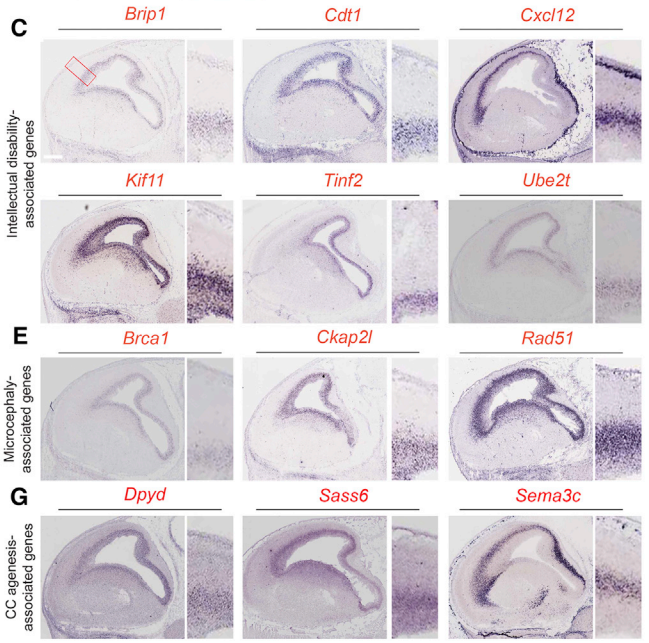

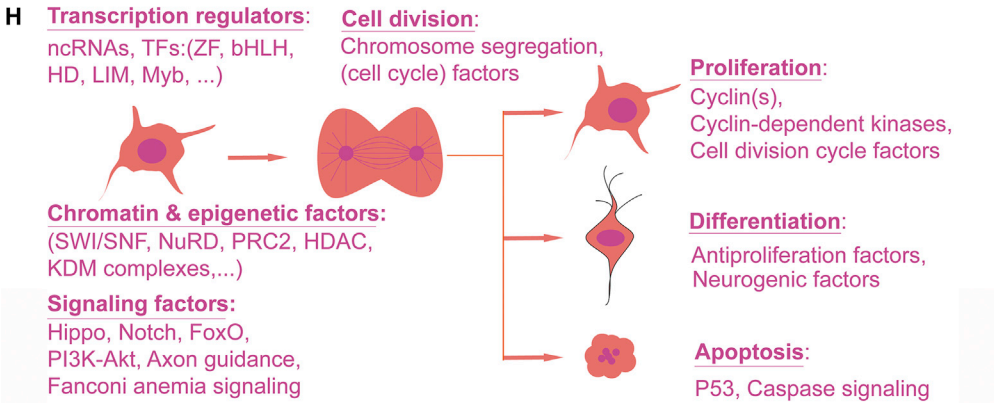

(legend on next page)

Given the reduction in the progenitor pool and death of differentiated neurons, we found a drastic decrease in the number of NEUN$^+$ or HuCD$^+$ neurons in the presumptive *Esco2*cKO cortex compared with control (Figure S6). Our observations are consistent with previous studies, which reported that cortical layers are not formed as a result of ESCO2 abolishment (Whelan et al., 2012b).

Together, this part of our investigation shows that *Esco2* is expressed in a subset of PAX6$^+$ RGCs and TBR2$^+$ IPCs in the developing cortex. The expression of *Esco2* is required for the viability of these cell populations and their progenies to afford proper cortical histogenesis.

ESCO2 Is Required for Maintenance of the IPC Population in Developing Cortex

Because the loss of ESCO2 in early cortical progenitors in transgenic *Esco2*cKO mutants caused massive apoptosis and cortical dysgenesis, we were limited in examining the role of ESCO2 at later stages of cortical development. Alternatively, an *in utero* electroporation (IUE) technique was employed to acutely delete *Esco2* from individual RGCs in the developing mouse cortex. The prominent expression of ESCO2 in IPCs and cells in the transition between RGCs and IPCs as well as the massive loss of these cell types following ablation of *Esco2* in the early developing cortex in *Esco2*cKO embryos prompted us to investigate whether ESCO2 influences the cell viability and generation of TBR2$^+$ IPCs from RGCs in late corticogenesis.

The brains of *Esco2*fl/fl embryos at E15.5 were electroporated either with pCIG2-Cre-ires-GFP (Cre-GFP) or control pCIG2-ires-GFP (GFP) plasmids. The cortices were harvested 30 h post electroporation (i.e., at E16.5) and processed for immunohistological analyses (Figures 7A and 7C). At mid-gestation, RGCs undergo only one division in less than 24 h to produce daughter cells, mainly IPCs in the developing mouse cortex (Noctor et al., 2004). To study the viability of apical progenitor daughter cells and the generation of IPCs from RGCs after deletion of *Esco2* in the VZ, we performed triple immunostaining for GFP/PAX6/CASP3 and GFP/TBR2/CASP3 at E16.5 (Figures 7A and 7C).

The electroporated (eGFP$^+$) cells mainly occupied the VZ and the basal half of the cortical wall (i.e., SVZ and intermediate zone [IZ]). In contrast to almost no CASP3$^+$ cells found in control (GFP) plasmid-injected cortex, many CASP3$^+$ apoptotic cells were seen in Cre-electroporated cortex as expected (Figures 7A and 7C). In the Cre-injected cortex, the majority of the GFP$^+$/CASP3$^+$ cells were found to be either negative (~80.0% ± 11.4%) or low (~17.6% ± 5.4%) for PAX6 expression (Figures 7A and 7B). On the other hand, the number of GFP$^+$/CASP3$^+$ cells expressing TBR2 was much higher (78.0% ± 9.7%) than those without TBR2 expression (Figures 7C and 7D). The findings further support the idea that expression of ESCO2 is required for TBR2$^+$ IPC viability and those of committed RGCs (with low PAX6 expression) to generate IPCs in both early and late cortical development.

Interestingly, there was no significant difference between the GFP- and Cre-GFP-electroporated cortex in terms of the number of transfected cells (GFP$^+$) expressing PAX6 or TBR2 (Figure 7E). Thus, ESCO2 is dispensable for the differentiation of RGCs, which are low in *Esco2* expression (Figures 7F and S5), into IPCs. This implies that following the acute deletion of *Esco2*, IPCs as progenies of PAX6-expressing RGCs are likely normally formed but fail to survive. It is also conceivable that NEUN$^+$ or HuCD$^+$ neurons that manage to differentiate from the ESCO2-deficient cortical neural progenitors, especially IPCs, are unhealthy and subsequently die via apoptosis (Figures 7F and S6).

Taking our data together, we show that ESCO2 expression is essential for the maintenance of IPCs and proper neurogenesis during cortical development.

DISCUSSION

Transcriptome analyses of molecularly sorted cells can enhance the identification of cell-type-specific factors, which can help us understand the molecular landscape in cell lineages. In this study, we report the molecular characterization of the evolutionarily and clinically important IPCs in the developing mouse cortex. We identified distinct sets of largely uncharacterized genes that exhibit enriched

Figure 5. Mutation of IPC Genes May Underlie Human Cortical Malformation and Intellectual Disability

(A) Graphical representation of human phenotype ontology for TBR2$^+$ IPCs genes showing the top ten phenotypes and others that follow in ranking.

(B, D, and F) List of the genes identified in IPCs with phenotypic implications for intellectual disabilities, microcephaly, and corpus callosum agenesis, respectively.

(C, E, and G) Respective array of micrographs showing *in situ* hybridization of examples of genes (highlighted red in the adjoining gene list) with distinctive expression in the developing mouse cortical subventricular zone, and whose dysfunction can lead to abnormal cortical structure and function. CC, corpus callosum. Magnified cortical region is shown by a red box in (C). Scale bar, 100 μm.

(H) Schema showing examples of regulatory factors involved in transcription regulation, signaling pathways in progenitor cells, and those involved in the cell cycle and chromosome segregation that drive cellular processes such as proliferation, differentiation, and apoptosis.

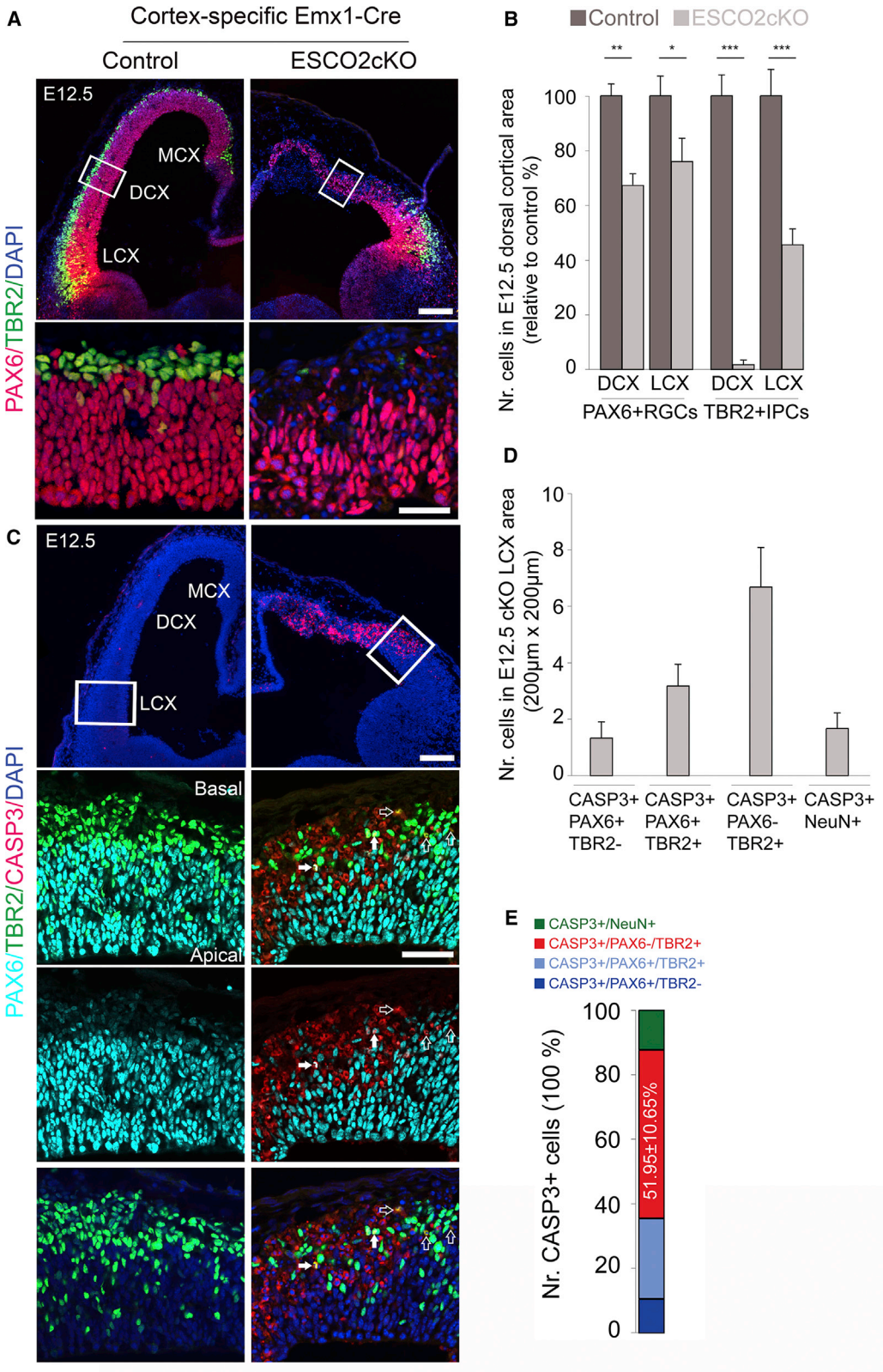

(legend on next page)

expression in IPCs among other cell types in the developing cortex. The set of genes were found to belong to transcription regulators, chromatin and epigenetic factors, signaling factors, and chromosome segregation (cell cycle) regulators. These genes encode critically important molecules for proper proliferation, differentiation, and maintenance of IPCs. Even though our understanding of the contribution of IPCs in cortical development has improved, several key questions remain enigmatic (Hevner, 2019). Our study represents the first comprehensive characterization of the molecular signature of IPCs in developing mouse cortex. The findings provide hints for future investigation to resolve the many unanswered questions.

Previous studies indicate that more than half of the IPC daughter cells undergo apoptosis during corticogenesis (Hevner, 2019; Mihalas and Hevner, 2018). The relevance of this phenomenon is undetermined; however, it might be associated with the regulation of the net neurogenic output, genome quality, neuronal subtype proportions during cortical development, and cortical evolution (Haydar et al., 1999; Hevner, 2019). The observed abundance of apoptotic cells among intermediate progenitor daughter cells harmonizes with previous reports documenting marked cell death in the SVZ and IZ of embryonic rodent cortex (Blaschke et al., 1996; Thomaidou et al., 1997). Along the same line of evidence, our GO analysis revealed that genes belonging to the caspase cascade in apoptosis are enriched in IPCs. Remarkably, disruption of the caspase cascade leads to decreased programmed cell death resulting in neuronal supernumerary, which likely accounts for the expansion and exencephaly of the forebrain, and cerebral gyrification (Kuida et al., 1996, 1998). Conversely, dysregulation of chromosomal segregation can cause an increase in neural progenitor cell death, leading to loss of neurons as exemplified in our *Esco2* case study. Thus, the proper coordination of the various aspects of the apoptosis signaling pathway, especially during embryonic neurogenesis, is essential for the determination of normal cortical size and form. Given the critical contribution of apoptosis to correct progression of cortical morphogenesis, it would be of great interest for future investigations to elucidate the precise mechanisms that trigger apoptotic cell death of neural cells during cortical development.

Notably, our validation investigations revealed that lack of *Esco2*, one of the identified IPC-enriched genes results in striking loss of IPCs, leading to the failure of proper formation of the cortex. By using different model systems such as yeast, primary mouse embryonic fibroblasts, and human cells (HeLa and 293T human embryonic kidney cells), previous studies reported that ESCO2 is crucial for sister chromatid tethering (Hou and Zou, 2005; Terret et al., 2009; Vega et al., 2005; Whelan et al., 2012a, 2012b). It is known to do so via its catalytic function in cohesin acetylation that ensures proper cohesion between sister chromatids. Indeed, dysfunction of ESCO2 has been shown to result in loss of cohesion at heterochromatic regions of centromeres, leading to defective localization of cohesin on chromosomes and apoptosis (Hou and Zou, 2005; Terret et al., 2009; Vega et al., 2005). In developing mouse cortex, a highly enriched expression of *Esco1* and *Esco2* was found in RGCs in VZ and in IPCs in SVZ, respectively. This suggests a possibility that the cohesin acetyltransferases ESCO1 and ESCO2 are key cell viability factors, which act by maintaining the appropriate cohesion in pericentric heterochromatin in RGC and IPC populations. Indeed, our findings indicate that ESCO2 is indispensable for IPC maintenance and demonstrate the identification of a central genetic determinant of IPC biogenesis in the developing mouse cortex.

In conclusion, our transcriptome data provide a crucial resource for further investigations aimed at understanding how IPC-related genetic factors contribute to cortical development and their implication for neurological disorders. Moreover, because IPCs are believed to be responsible for a large portion of mammalian corticogenesis, and the size of the IPC-laden SVZ correlates with brain phylogeny, future studies can look into the role of the identified IPC genes in cortical evolution.

Figure 6. Lack of ESCO2 Causes Apoptosis of Cortical Progenitors Leading to Disturbance of Cortical Development

(A) Micrographs showing low and high magnification of the E12.5 control (wild-type) and *Esco2* cKO cortex immunostained for PAX6 and TBR2. The medial (MCX), dorsal (DCX), and lateral (LCX) aspects of the cortex are indicated. Counterstaining was done with DAPI.

(B) Bar graph showing quantification of $PAX6^+$ and $TBR2^+$ cells in the E12.5 control and *Esco2* cKO dorsal cortical area marked with a white box in (A).

(C) Micrographs showing low and high magnification of the E12.5 control and *Esco2* cKO cortex immunostained for PAX6, TBR2, and the apoptosis marker CASP3. Counterstaining was done with DAPI. The medial (MCX), dorsal (DCX), and lateral (LCX) aspects of the cortex are indicated. The basal and apical sides of the cortex are shown. Filled arrows point to $PAX6^+/TBR2^+$ cells, which are in transition stage between RGCs and IPCs, undergoing apoptosis ($CASP3^+$), whereas empty arrows point to apoptotic ($CASP3^+$) $TBR2^+$ IPCs.

(D and E) Bar graph (D) showing quantification of the number of $PAX6^+$, $TBR2^+$, $PAX6/TBR2^+$, or $NEUN^+$ cells undergoing apoptosis, and composite bar graph (E) showing the quantitative proportion of $CASP3^+$ cells co-expressing PAX6 or TBR2 or NEUN in the lateral cortex (marked with white box in C). Error bars are SEM.

*$p < 0.05$, **$p < 0.01$, ***$p < 0.001$. Experimental replicates (n) = 4 (B) and 6 (D and E). Scale bars, 50 μm (lower panels in A and C) and 200 μm (upper panels in A and C).

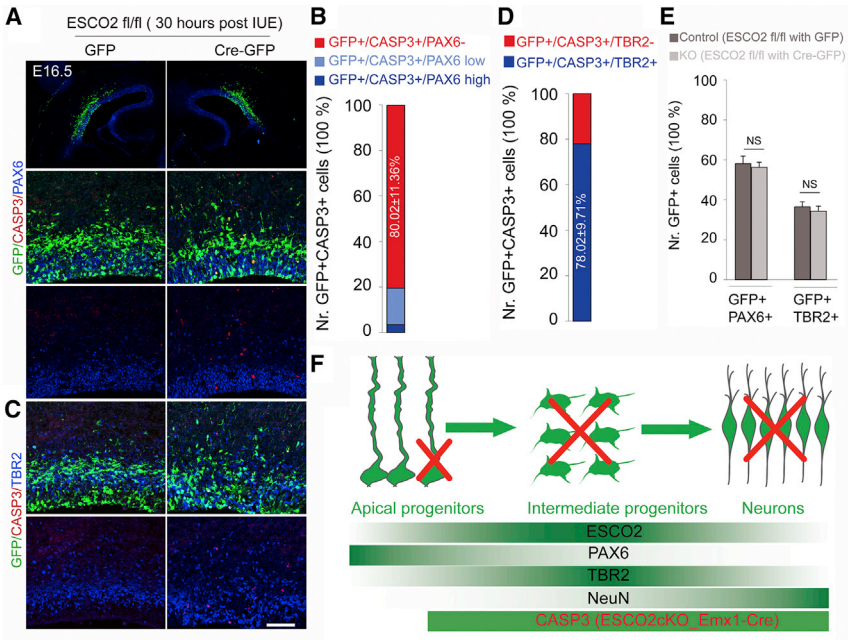

Figure 7. Expression of ESCO2 Is Important for Maintenance but Not Generation of IPCs

(A and C) Micrographs at low and high magnification showing GFP, CASP3, and PAX6 (A) or TBR2 (C) immunostaining in the E16.5 *Esco2*fl/fl mouse cortex electroporated with a GFP-only plasmid as control and GFP-Cre plasmid to delete *Esco2* in the transfected cells.

(B and D) Composite bar graphs showing quantitative analysis of the proportion of GFP and CASP3 positive cells with either no/low/high PAX6 expression (B) or with/without TBR2 expression (D).

(E) Bar graphs showing no significant difference between the total number of cells co-expressing GFP and PAX6 or GFP and TBR2 when the control (GFP-only) and knockout (GFP-Cre) cortices are compared. Error bars are SEM.

(F) Schema illustrating the expression of PAX6, TBR2, NEUN, and ESCO2 during differentiation of radial glial progenitors to intermediate progenitors and neurons. The loss of ESCO2 in *Esco2*cKO_Emx1-Cre seems to cause apoptosis in the late radial glial progenitors ($PAX6^+/TBR2^+$), intermediate progenitors ($TBR2^+$), and neurons (NEUN).

NS, not significant. Experimental replicates (n) = 6 (B, D, E). Scale bar, 50 μm.

EXPERIMENTAL PROCEDURES

$TBR2^+$ Nuclei Sorting Protocol for Transcriptomic Data Generation from Embryonic Mouse Brain

Cells expressing TBR2 in the E16.5 mouse cortex were isolated by FACS and profiled using RNA sequencing. The detailed protocol is reported in Sakib et al. (2021). The experiment was carried out using three biological replicates.

RNA Sequencing and Bioinformatics Analysis

Sorted nuclei were collected into non-specific binding coated Falcon tubes and pelleted via brief centrifugation, and the RNA was isolated using a TRIzol LS (Invitrogen) protocol along with aqueous phase cleanup using a Zymo RNA Clean & Concentrator-5 kit. RNA-seq libraries were prepared using a Takara SMART-Seq v4 Ultra Low Input RNA kit using 1 ng of RNA according to the manufacturer's protocol. Base calling, fastq conversion, quality control, and read alignments were all performed as outlined previously (Narayanan et al., 2015; Nguyen et al., 2018). Reads were aligned to mouse genome mm10 and counted using FeaturesCount (http://bioinf.wehi.edu.au/featureCounts/). Further descriptions of informatics analyses are provided in supplemental experimental procedures.

Transgenic Mice and *In Utero* Electroporation

Floxed *Esco2* (Whelan et al., 2012b) and *Emx1-Cre* (Gorski et al., 2002) mice were maintained in a C57BL6/J background. Animals were handled according to the German Animal Protection Law. IUE was performed as described previously (Tuoc and Stoykova, 2008; Tuoc et al., 2013).

Plasmids and Antibodies

A list of plasmids and antibodies with detailed descriptions is provided in supplemental experimental procedures.

Immunohistochemistry and *In Situ* Hybridization Validation

Immunohistochemistry (IHC) and ISH were performed as previously described (Bachmann et al., 2016; Tuoc et al., 2013; Visel et al., 2004). In brief, sections for IHC were incubated overnight with primary antibody at 4°C after blocking with normal sera of the appropriate species. Primary antibodies were detected with a fluorescent secondary antibody (Alexa Fluor, 1:400; Invitrogen). Sections were later counterstained with Vectashield mounting medium containing DAPI (4′,6-diamidino-2-phenylindole; Vector Laboratories) to label nuclei.

A detail ISH protocol with different conditions was described in our previous study (Visel et al., 2004) and can be found in our online digital atlas (https://gp3.mpg.de). The template sequence and ISH conditions are described in the webpage for each gene.

Imaging, Quantification, Statistical Analysis, and Data Availability

Micrographs were obtained by confocal fluorescence microscopy (TCS SP5, Leica) and analyzed using an Axio Imager M2 (Zeiss) with a Neurolucida system. Images were processed further using Adobe Photoshop. The statistical quantification was carried out as average from at least three biological replicates. Detailed statistical analyses and descriptions of histological experiments are presented in Table S8. The *in situ* expressions of all the identified

IPC genes are freely available online (https://gp3.mpg.de) in an interactive database.

Accession Numbers

All RNA-seq data have been deposited in the Gene Expression Omnibus under accession number GEO: GSE168298.

SUPPLEMENTAL INFORMATION

Supplemental Information can be found online at https://doi.org/10.1016/j.stemcr.2021.03.008.

AUTHOR CONTRIBUTIONS

M.S.S., C.K., and A.F. established TBR2^{+} cell sorting and RNA-seq. P.A.U., L.P., G.S., Y.X., J.R., and X.M. analyzed RNA-seq data and mouse phenotype. P.D. and G.E. contributed to generation of *Esco2*cKO line and histological analysis, and provided ISH data. J.F.S., G.E., U.T., A.F., H.P.N. provided research tools and offered discussions for the study. T.T. conceived the study. T.T. and G.S. wrote the manuscript.

DECLARATION OF INTERESTS

The authors declare no competing interests.

ACKNOWLEDGMENTS

We acknowledge U. Kunze and C. Heuchel for their expert animal care. We thank K. Jones for providing reagents and M. Witte for helpful discussions. This work was supported by TU432/1-1, TU432/3-1, TU432/6-1 DFG grants (T.T.), and Schram-Stiftung (T.T.). A.F. was supported by the DZNE, the ERC consolidator grant DEPICODE (648898), SFB1286. and the DFG under Germany's Excellence Strategy-EXC 2067/1390729940.

Received: August 13, 2020
Revised: March 5, 2021
Accepted: March 8, 2021
Published: April 1, 2021

REFERENCES

Albert, M., Kalebic, N., Florio, M., Lakshmanaperumal, N., Haffner, C., Brandl, H., Henry, I., and Huttner, W.B. (2017). Epigenome profiling and editing of neocortical progenitor cells during development. EMBO J. *36*, 2642–2658.

Amamoto, R., Zuccaro, E., Curry, N.C., Khurana, S., Chen, H.H., Cepko, C.L., and Arlotta, P. (2020). FIN-Seq: transcriptional profiling of specific cell types from frozen archived tissue of the human central nervous system. Nucleic Acids Res. *48*, e4.

Arlotta, P., Molyneaux, B.J., Chen, J., Inoue, J., Kominami, R., and Macklis, J.D. (2005). Neuronal subtype-specific genes that control corticospinal motor neuron development in vivo. Neuron *45*, 207–221.

Arnold, S.J., Huang, G.J., Cheung, A.F., Era, T., Nishikawa, S., Bikoff, E.K., Molnar, Z., Robertson, E.J., and Groszer, M. (2008). The T-box transcription factor Eomes/Tbr2 regulates neurogenesis in the cortical subventricular zone. Genes Dev. *22*, 2479–2484.

Baala, L., Briault, S., Etchevers, H.C., Laumonnier, F., Natiq, A., Amiel, J., Boddaert, N., Picard, C., Sbiti, A., Asermouh, A., et al. (2007). Homozygous silencing of T-box transcription factor EOMES leads to microcephaly with polymicrogyria and corpus callosum agenesis. Nat. Genet. *39*, 454–456.

Bachmann, C., Nguyen, H., Rosenbusch, J., Pham, L., Rabe, T., Patwa, M., Sokpor, G., Seong, R.H., Ashery-Padan, R., Mansouri, A., et al. (2016). mSWI/SNF (BAF) complexes are indispensable for the neurogenesis and development of embryonic olfactory epithelium. PLoS Genet. *12*, e1006274.

Blaschke, A.J., Staley, K., and Chun, J. (1996). Widespread programmed cell death in proliferative and postmitotic regions of the fetal cerebral cortex. Development *122*, 1165–1174.

Fan, X., Dong, J., Zhong, S., Wei, Y., Wu, Q., Yan, L., Yong, J., Sun, L., Wang, X., Zhao, Y., et al. (2018). Spatial transcriptomic survey of human embryonic cerebral cortex by single-cell RNA-seq analysis. Cell Res. *28*, 730–745.

Gorski, J.A., Talley, T., Qiu, M., Puelles, L., Rubenstein, J.L., and Jones, K.R. (2002). Cortical excitatory neurons and glia, but not GABAergic neurons, are produced in the Emx1-expressing lineage. J. Neurosci. *22*, 6309–6314.

Haubensak, W., Attardo, A., Denk, W., and Huttner, W.B. (2004). Neurons arise in the basal neuroepithelium of the early mammalian telencephalon: a major site of neurogenesis. Proc. Natl. Acad. Sci. U S A *101*, 3196–3201.

Haydar, T.F., Kuan, C.Y., Flavell, R.A., and Rakic, P. (1999). The role of cell death in regulating the size and shape of the mammalian forebrain. Cereb. Cortex *9*, 621–626.

Hevner, R.F. (2019). Intermediate progenitors and Tbr2 in cortical development. J. Anat. *235*, 616–625.

Hou, F., and Zou, H. (2005). Two human orthologues of Eco1/Ctf7 acetyltransferases are both required for proper sister-chromatid cohesion. Mol. Biol. Cell *16*, 3908–3918.

Kawaguchi, A., Ikawa, T., Kasukawa, T., Ueda, H.R., Kurimoto, K., Saitou, M., and Matsuzaki, F. (2008). Single-cell gene profiling defines differential progenitor subclasses in mammalian neurogenesis. Development *135*, 3113–3124.

Kostic, M., Paridaen, J., Long, K.R., Kalebic, N., Langen, B., Grubling, N., Wimberger, P., Kawasaki, H., Namba, T., and Huttner, W.B. (2019). YAP activity is necessary and sufficient for basal progenitor abundance and proliferation in the developing neocortex. Cell Rep. *27*, 1103–1118 e1106.

Kowalczyk, T., Pontious, A., Englund, C., Daza, R.A., Bedogni, F., Hodge, R., Attardo, A., Bell, C., Huttner, W.B., and Hevner, R.F. (2009). Intermediate neuronal progenitors (basal progenitors) produce pyramidal-projection neurons for all layers of cerebral cortex. Cereb. Cortex *19*, 2439–2450.

Kuida, K., Haydar, T.F., Kuan, C.Y., Gu, Y., Taya, C., Karasuyama, H., Su, M.S., Rakic, P., and Flavell, R.A. (1998). Reduced apoptosis and cytochrome c-mediated caspase activation in mice lacking caspase 9. Cell *94*, 325–337.

Kuida, K., Zheng, T.S., Na, S., Kuan, C., Yang, D., Karasuyama, H., Rakic, P., and Flavell, R.A. (1996). Decreased apoptosis in the brain and premature lethality in CPP32-deficient mice. Nature *384*, 368–372.

Li, M., Santpere, G., Imamura Kawasawa, Y., Evgrafov, O.V., Gulden, F.O., Pochareddy, S., Sunkin, S.M., Li, Z., Shin, Y., Zhu, Y., et al. (2018). Integrative functional genomic analysis of human brain development and neuropsychiatric risks. Science *362*, eaat7615.

Li, Z., Tyler, W.A., Zeldich, E., Santpere Baro, G., Okamoto, M., Gao, T., Li, M., Sestan, N., and Haydar, T.F. (2020). Transcriptional priming as a conserved mechanism of lineage diversification in the developing mouse and human neocortex. Sci. Adv. *6*, eabd2068.

Liu, S.J., Nowakowski, T.J., Pollen, A.A., Lui, J.H., Horlbeck, M.A., Attenello, F.J., He, D., Weissman, J.S., Kriegstein, A.R., Diaz, A.A., et al. (2016). Single-cell analysis of long non-coding RNAs in the developing human neocortex. Genome Biol. *17*, 67.

Loo, L., Simon, J.M., Xing, L., McCoy, E.S., Niehaus, J.K., Guo, J., Anton, E.S., and Zylka, M.J. (2019). Single-cell transcriptomic analysis of mouse neocortical development. Nat. Commun. *10*, 134.

Mihalas, A.B., Elsen, G.E., Bedogni, F., Daza, R.A.M., Ramos-Laguna, K.A., Arnold, S.J., and Hevner, R.F. (2016). Intermediate progenitor cohorts differentially generate cortical layers and require Tbr2 for timely acquisition of neuronal subtype identity. Cell Rep. *16*, 92–105.

Mihalas, A.B., and Hevner, R.F. (2018). Clonal analysis reveals laminar fate multipotency and daughter cell apoptosis of mouse cortical intermediate progenitors. Development *145*, dev164335.

Miyata, T., Kawaguchi, A., Saito, K., Kawano, M., Muto, T., and Ogawa, M. (2004). Asymmetric production of surface-dividing and non-surface-dividing cortical progenitor cells. Development *131*, 3133–3145.

Molyneaux, B.J., Goff, L.A., Brettler, A.C., Chen, H.H., Hrvatin, S., Rinn, J.L., and Arlotta, P. (2015). DeCoN: genome-wide analysis of in vivo transcriptional dynamics during pyramidal neuron fate selection in neocortex. Neuron *85*, 275–288.

Narayanan, R., Pirouz, M., Kerimoglu, C., Pham, L., Wagener, R.J., Kiszka, K.A., Rosenbusch, J., Seong, R.H., Kessel, M., Fischer, A., et al. (2015). Loss of BAF (mSWI/SNF) complexes causes global transcriptional and chromatin state changes in forebrain development. Cell Rep. *13*, 1842–1854.

Nguyen, H., Kerimoglu, C., Pirouz, M., Pham, L., Kiszka, K.A., Sokpor, G., Sakib, M.S., Rosenbusch, J., Teichmann, U., Seong, R.H., et al. (2018). Epigenetic regulation by BAF complexes limits neural stem cell proliferation by suppressing wnt signaling in late embryonic development. Stem Cell Rep. *10*, 1734–1750.

Nishiyama, T., Ladurner, R., Schmitz, J., Kreidl, E., Schleiffer, A., Bhaskara, V., Bando, M., Shirahige, K., Hyman, A.A., Mechtler, K., et al. (2010). Sororin mediates sister chromatid cohesion by antagonizing Waal. Cell *143*, 737–749.

Noctor, S.C., Martinez-Cerdeno, V., Ivic, L., and Kriegstein, A.R. (2004). Cortical neurons arise in symmetric and asymmetric division zones and migrate through specific phases. Nat. Neurosci. *7*, 136–144.

Nowakowski, T.J., Bhaduri, A., Pollen, A.A., Alvarado, B., Mostajo-Radji, M.A., Di Lullo, E., Haeussler, M., Sandoval-Espinosa, C., Liu, S.J., Velmeshev, D., et al. (2017). Spatiotemporal gene expression trajectories reveal developmental hierarchies of the human cortex. Science *358*, 1318–1323.

Ouyang, T., Meng, W., Li, M., Hong, T., and Zhang, N. (2020). Recent advances of the Hippo/YAP signaling pathway in brain development and glioma. Cell. Mol. Neurobiol. *40*, 495–510.

Pinto, L., Mader, M.T., Irmler, M., Gentilini, M., Santoni, F., Drechsel, D., Blum, R., Stahl, R., Bulfone, A., Malatesta, P., et al. (2008). Prospective isolation of functionally distinct radial glial subtypes—lineage and transcriptome analysis. Mol. Cell. Neurosci. *38*, 15–42.

Pollen, A.A., Nowakowski, T.J., Chen, J., Retallack, H., Sandoval-Espinosa, C., Nicholas, C.R., Shuga, J., Liu, S.J., Oldham, M.C., Diaz, A., et al. (2015). Molecular identity of human outer radial glia during cortical development. Cell *163*, 55–67.

Robinson, P.N., Kohler, S., Bauer, S., Seelow, D., Horn, D., and Mundlos, S. (2008). The Human Phenotype Ontology: a tool for annotating and analyzing human hereditary disease. Am. J. Hum. Genet. *83*, 610–615.

Rolef Ben-Shahar, T., Heeger, S., Lehane, C., East, P., Flynn, H., Skehel, M., and Uhlmann, F. (2008). Eco1-dependent cohesin acetylation during establishment of sister chromatid cohesion. Science *321*, 563–566.

Sakib, M.S., Sokpor, G., Nguyen, H.P., Fischer, A., and Tuoc, T. (2021). Intranuclear immunostaining-based FACS protocol from embryonic cortical tissue. STAR Protoc. *2*, 100318.

Sessa, A., Mao, C.A., Hadjantonakis, A.K., Klein, W.H., and Broccoli, V. (2008). Tbr2 directs conversion of radial glia into basal precursors and guides neuronal amplification by indirect neurogenesis in the developing neocortex. Neuron *60*, 56–69.

Telley, L., Govindan, S., Prados, J., Stevant, I., Nef, S., Dermitzakis, E., Dayer, A., and Jabaudon, D. (2016). Sequential transcriptional waves direct the differentiation of newborn neurons in the mouse neocortex. Science *351*, 1443–1446.

Terret, M.E., Sherwood, R., Rahman, S., Qin, J., and Jallepalli, P.V. (2009). Cohesin acetylation speeds the replication fork. Nature *462*, 231–234.

Thomaidou, D., Mione, M.C., Cavanagh, J.F., and Parnavelas, J.G. (1997). Apoptosis and its relation to the cell cycle in the developing cerebral cortex. J. Neurosci. *17*, 1075–1085.

Tuoc, T.C., and Stoykova, A. (2008). Trim11 modulates the function of neurogenic transcription factor Pax6 through ubiquitin-proteosome system. Gene Dev *22*, 1972–1986.

Tuoc, T.C., Boretius, S., Sansom, S.N., Pitulescu, M.E., Frahm, J., Livesey, F.J., and Stoykova, A. (2013). Chromatin regulation by BAF170 controls cerebral cortical size and thickness. Dev. Cell *25*, 256–269.

Unal, E., Heidinger-Pauli, J.M., Kim, W., Guacci, V., Onn, I., Gygi, S.P., and Koshland, D.E. (2008). A molecular determinant for the establishment of sister chromatid cohesion. Science *321*, 566–569.

Vega, H., Waisfisz, Q., Gordillo, M., Sakai, N., Yanagihara, I., Yamada, M., van Gosliga, D., Kayserili, H., Xu, C., Ozono, K., et al. (2005). Roberts syndrome is caused by mutations in ESCO2, a human homolog of yeast ECO1 that is essential for the establishment of sister chromatid cohesion. Nat. Genet. *37*, 468–470.

Visel, A., Thaller, C., and Eichele, G. (2004). GenePaint.org: an atlas of gene expression patterns in the mouse embryo. Nucleic Acids Res. *32*, D552–D556.

Whelan, G., Kreidl, E., Peters, J.M., and Eichele, G. (2012a). The non-redundant function of cohesin acetyltransferase Esco2: some answers and new questions. Nucleus *3*, 330–334.

Whelan, G., Kreidl, E., Wutz, G., Egner, A., Peters, J.M., and Eichele, G. (2012b). Cohesin acetyltransferase Esco2 is a cell viability factor and is required for cohesion in pericentric heterochromatin. EMBO J. *31*, 71–82.

Zheng, Y., and Pan, D. (2019). The Hippo signaling pathway in development and disease. Dev. Cell *50*, 264–282.

Zhong, S., Zhang, S., Fan, X., Wu, Q., Yan, L., Dong, J., Zhang, H., Li, L., Sun, L., Pan, N., et al. (2018). A single-cell RNA-seq survey of the developmental landscape of the human prefrontal cortex. Nature *555*, 524–528.

Stem Cell Reports, Volume *16*

Supplemental Information

Molecular Profiling Reveals Involvement of ESCO2 in Intermediate Progenitor Cell Maintenance in the Developing Mouse Cortex

Pauline Antonie Ulmke, M. Sadman Sakib, Peter Ditte, Godwin Sokpor, Cemil Kerimoglu, Linh Pham, Yuanbin Xie, Xiaoyi Mao, Joachim Rosenbusch, Ulrike Teichmann, Huu Phuc Nguyen, Andre Fischer, Gregor Eichele, Jochen F. Staiger, and Tran Tuoc

SUPPLEMENTAL DATA

Figure S1

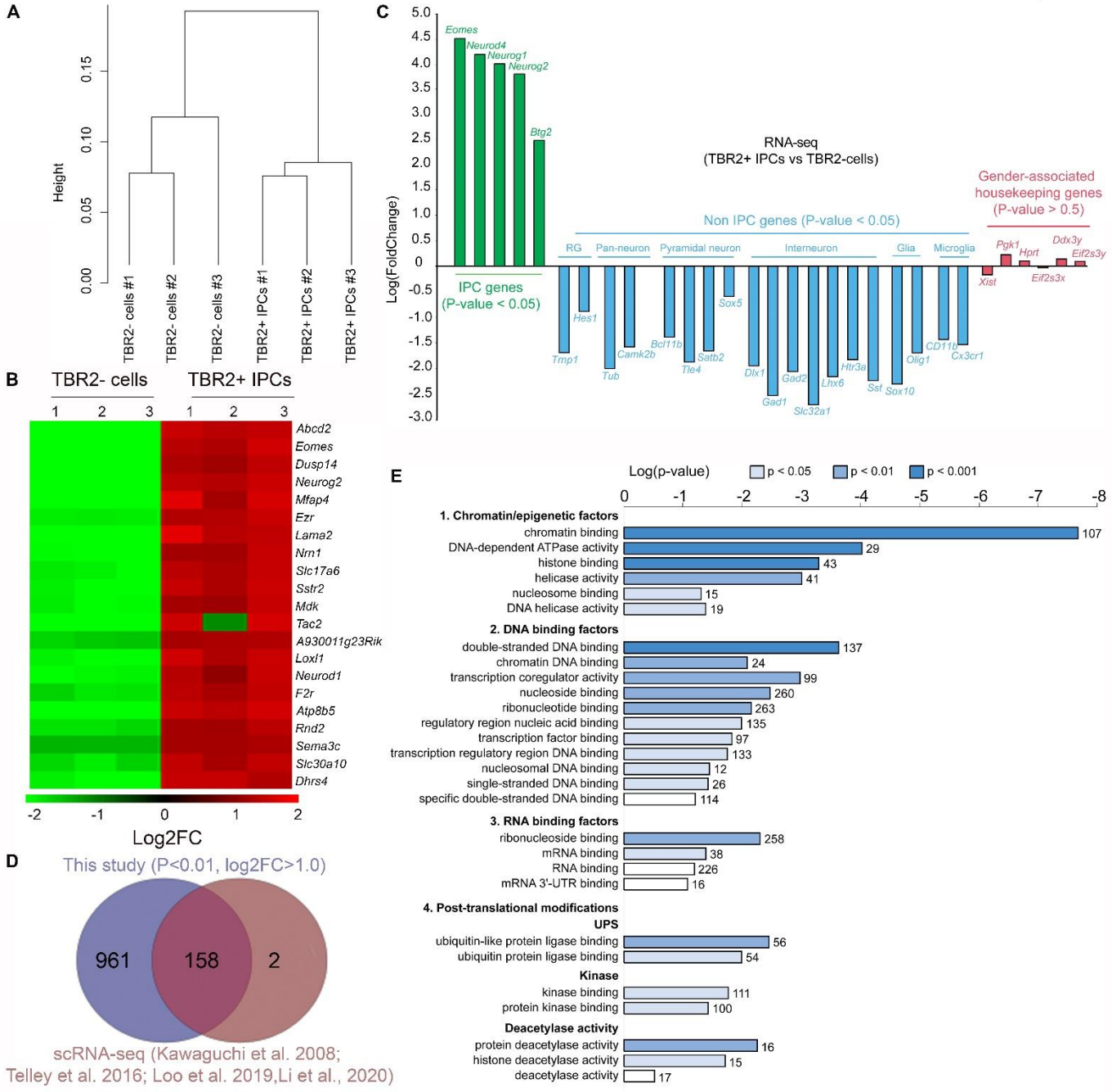

Figure S1 (related to figure 1). RNA-seq analysis of mouse TBR2+ IPCs and TBR2- cells. (A) Cluster dendrogram analysis of RNA-seq for TBR2+ and TBR2- sorted cell samples. (B) Heatmap showing the top 20 genes with high expression (enriched/upregulated) in TBR2+ IPCs and low expression in TBR2- cells. (C) Bar graph showing expression of selected IPC (in green), non-IPC (in blue) and gender-associated housekeeping genes (in red) in IPCs (TBR2+) and non IPCs (TBR2-) in the E16.5 mouse cortex. (D) An indication of the increased number of IPC-enriched genes identified in our study compared with previous studies performed at the IP single cell level. (E) Bar graph showing the molecular pathway analysis in TBR2+ IPCs and the number of genes belonging to each category of pathway.

Figure S2

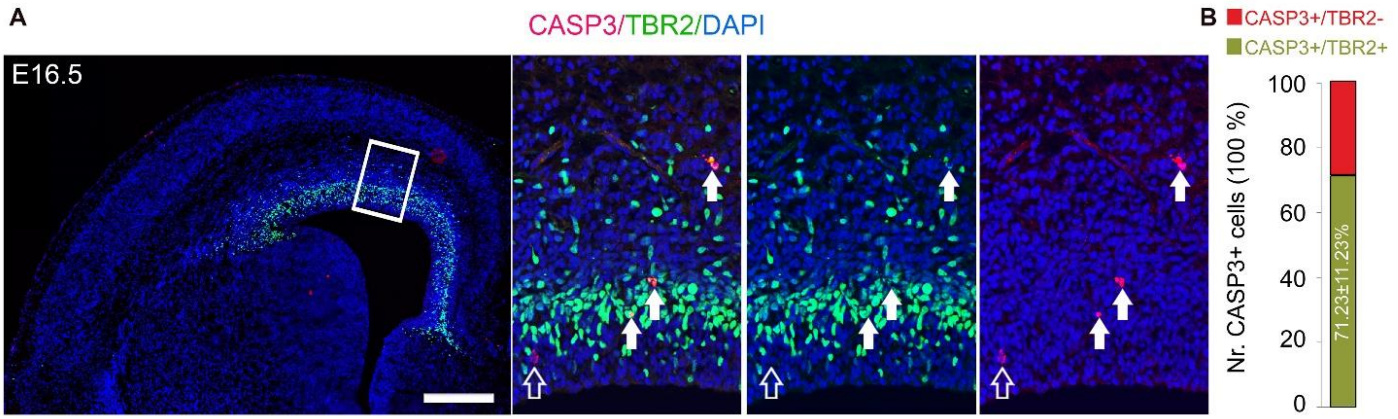
A
CASP3/TBR2/DAPI
E16.5
B
CASP3+/TBR2-
CASP3+/TBR2+
Nr. CASP3+ cells (100 %)
100
80
60
40
20
0
71.23±11.23%

Figure S2 (related to figure 3). TBR2+ IPCs in mouse display prominent apoptotic activity. (A) Immunohistochemical micrographs showing an overview of E16.5 mouse cortex and highly magnified germinal zone stained with TBR2 and CASP3 antibodies. The zoomed area is indicated with white inserted box. Filled arrows point to TBR2+ IPCs undergoing apoptosis whereas empty arrow indicates apoptotic activity in a TBR2- cell. Counterstaining was done with DAPI. (B) Bar graph showing the proportion of TBR2+ and TBR2- cells undergoing apoptosis. Experimental replicates (n) = 6 (B). Scale bar = 100 µm.

Figure S3

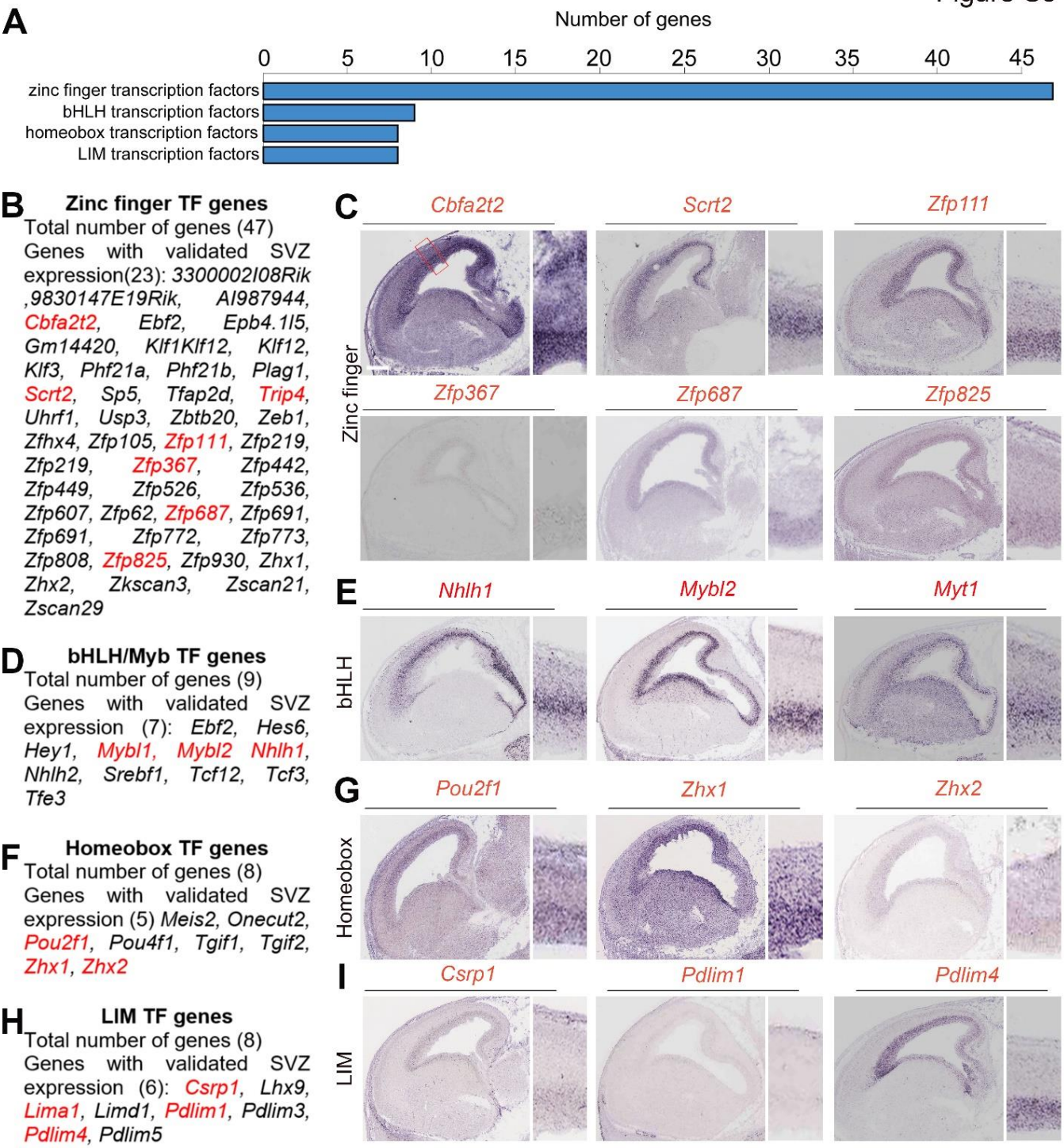
A
Number of genes
0 5 10 15 20 25 30 35 40 45
zinc finger transcription factors
bHLH transcription factors
homeobox transcription factors
LIM transcription factors
B
Zinc finger TF genes
Total number of genes (47)
Genes with validated SVZ expression(23): 3300002I08Rik ,9830147E19Rik, AI987944, Cbfa2t2, Ebf2, Epb4.1l5, Gm14420, Klf1Klf12, Klf12, Klf3, Phf21a, Phf21b, Plag1, Scrt2, Sp5, Tfap2d, Trip4, Uhrf1, Usp3, Zbtb20, Zeb1, Zfhx4, Zfp105, Zfp111, Zfp219, Zfp219, Zfp367, Zfp442, Zfp449, Zfp526, Zfp536, Zfp607, Zfp62, Zfp687, Zfp691, Zfp691, Zfp772, Zfp773, Zfp808, Zfp825, Zfp930, Zhx1, Zhx2, Zkscan3, Zscan21, Zscan29
D
bHLH/Myb TF genes
Total number of genes (9)
Genes with validated SVZ expression (7): Ebf2, Hes6, Hey1, Mybl1, Mybl2 Nhlh1, Nhlh2, Srebf1, Tcf12, Tcf3, Tfe3
F
Homeobox TF genes
Total number of genes (8)
Genes with validated SVZ expression (5) Meis2, Onecut2, Pou2f1, Pou4f1, Tgif1, Tgif2, Zhx1, Zhx2
H
LIM TF genes
Total number of genes (8)
Genes with validated SVZ expression (6): Csrp1, Lhx9, Lima1, Limd1, Pdlim1, Pdlim3, Pdlim4, Pdlim5
C
Cbfa2t2
Scrt2
Zfp111
Zinc finger
Zfp367
Zfp687
Zfp825
E
Nhlh1
Mybl2
Myt1
bHLH
G
Pou2f1
Zhx1
Zhx2
Homeobox
I
Csrp1
Pdlim1
Pdlim4
LIM

Figure S3 (related to figure 4). Enrichment of transcription factor genes in TBR2+ IPCs. (A) Bar graph showing the number of genes in IPCs under the indicated classes of transcription factor. (B, D, F, H) Categories of transcription factors with corresponding list of newly identified IPC-enriched genes. (C, E, G, I) Respective micrographs showing *in situ* hybridization of examples of the identified transcription factor genes (highlighted red in the adjoining gene list) with expression endowment in the developing mouse cortical subventricular zone. Magnified cortical region is shown with red box in (C). Scale bar = 100 µm.

Figure S4

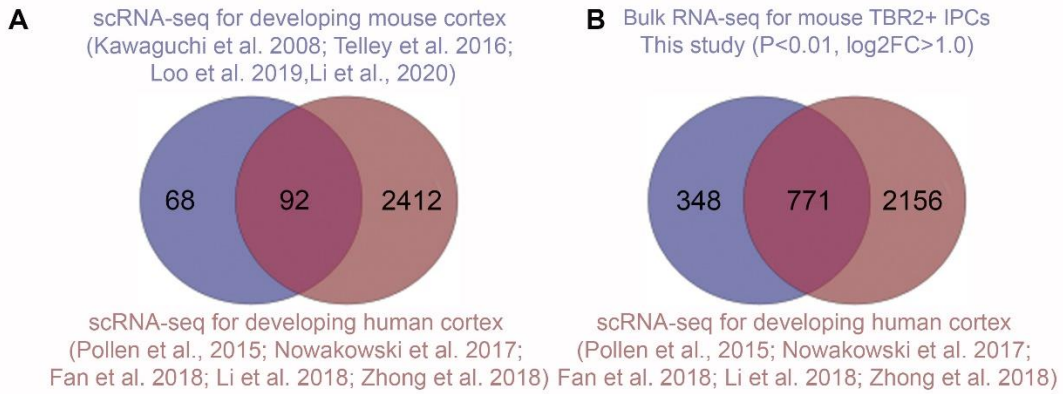
A
scRNA-seq for developing mouse cortex
(Kawaguchi et al. 2008; Telley et al. 2016;
Loo et al. 2019,Li et al., 2020)
68
92
2412
scRNA-seq for developing human cortex
(Pollen et al., 2015; Nowakowski et al. 2017;
Fan et al. 2018; Li et al. 2018; Zhong et al. 2018)
B
Bulk RNA-seq for mouse TBR2+ IPCs
This study (P<0.01, log2FC>1.0)
348
771
2156
scRNA-seq for developing human cortex
(Pollen et al., 2015; Nowakowski et al. 2017;
Fan et al. 2018; Li et al. 2018; Zhong et al. 2018)

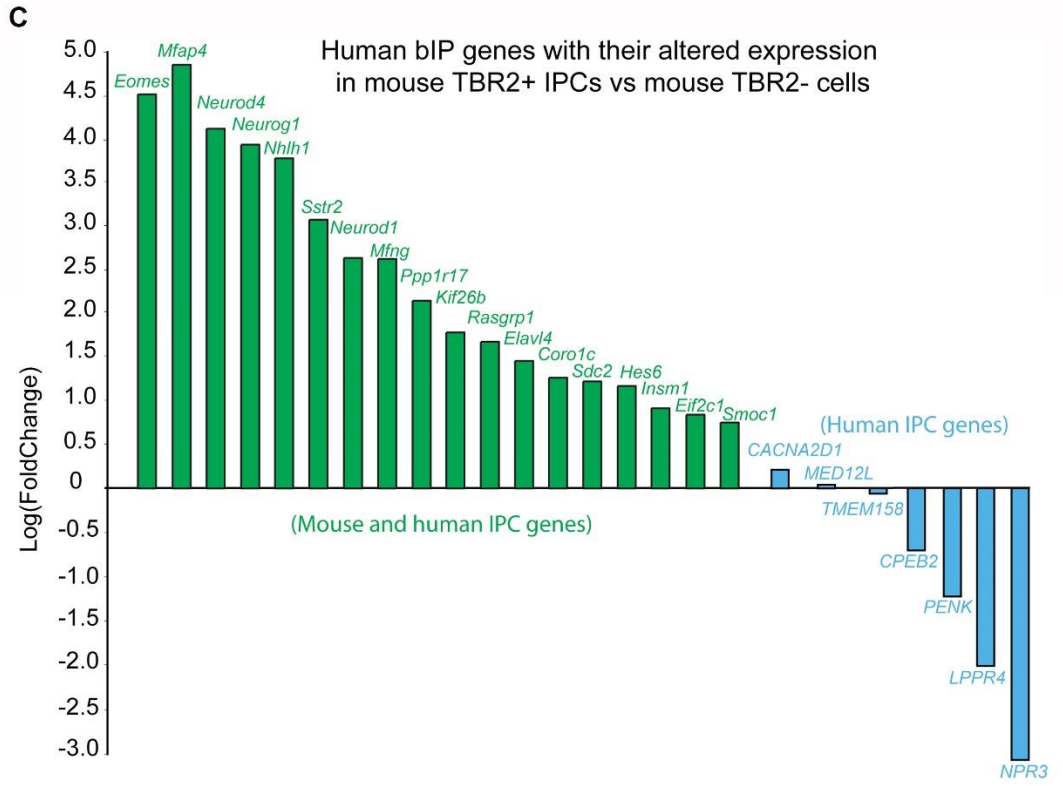
C
Human bIP genes with their altered expression
in mouse TBR2+ IPCs vs mouse TBR2- cells
Log(FoldChange)
5.0
4.5
4.0
3.5
3.0
2.5
2.0
1.5
1.0
0.5
0
-0.5
-1.0
-1.5
-2.0
-2.5
-3.0
Mfap4
Eomes
Neurod4
Neurog1
Nhlh1
Sstr2
Neurod1
Mfng
Ppp1r17
Kif26b
Rasgrp1
Elavl4
Coro1c
Sdc2
Hes6
Insm1
Eif2c1
Smoc1
CACNA2D1
MED12L
TMEM158
CPEB2
PENK
LPPR4
NPR3
(Mouse and human IPC genes)
(Human IPC genes)

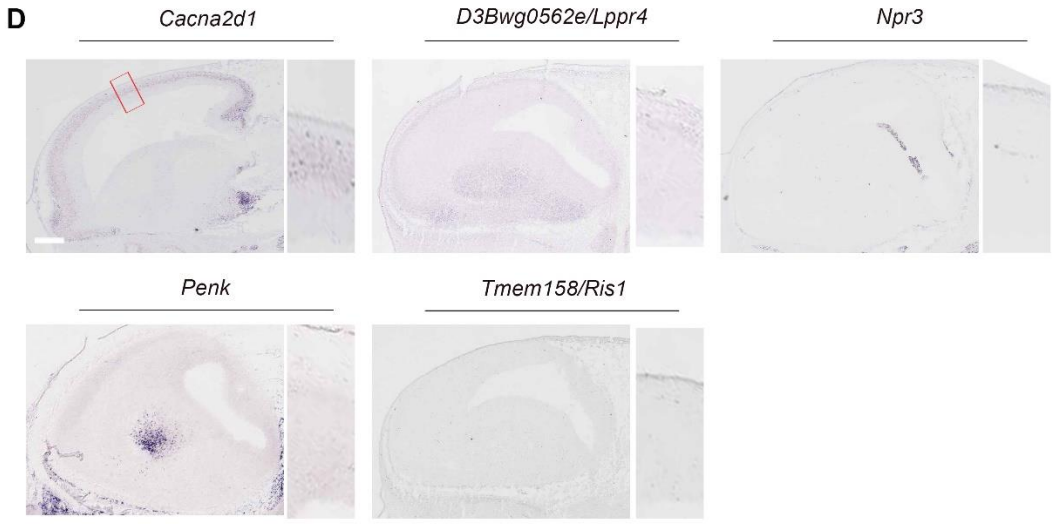
D
Cacna2d1
D3Bwg0562e/Lppr4
Npr3
Penk
Tmem158/Ris1

Figure S4 (related to figure 5). Many human bIP genes are upregulated in mouse TBR2+ IPCs while others are downregulated or absent. (A, B) Overlap between the number of human IPC genes from scRNA-seq analysis of the human developing cortex (Fan et al., 2018; Li et al., 2018; Nowakowski et al., 2017; Pollen et al., 2015; Zhong et al., 2018) and number of mouse IPC genes, which was recently identified by scRNA-seq analysis (Kawaguchi et al., 2008; Li et al., 2020; Loo et al., 2019; Telley et al., 2016) (A), and by bulk RNA-seq (B, this study). (C) Bar graph showing both upregulated (enriched) and downregulated human bIP genes in TBR2+ IPCs compared with TBR2- cells in mouse cortex. (D) *In situ* hybridization micrographs showing the E14.5 mouse cortex riboprobed for the indicated human bIP genes. Magnified cortical region is shown with red box. Scale bar = 100 µm.

Figure S5

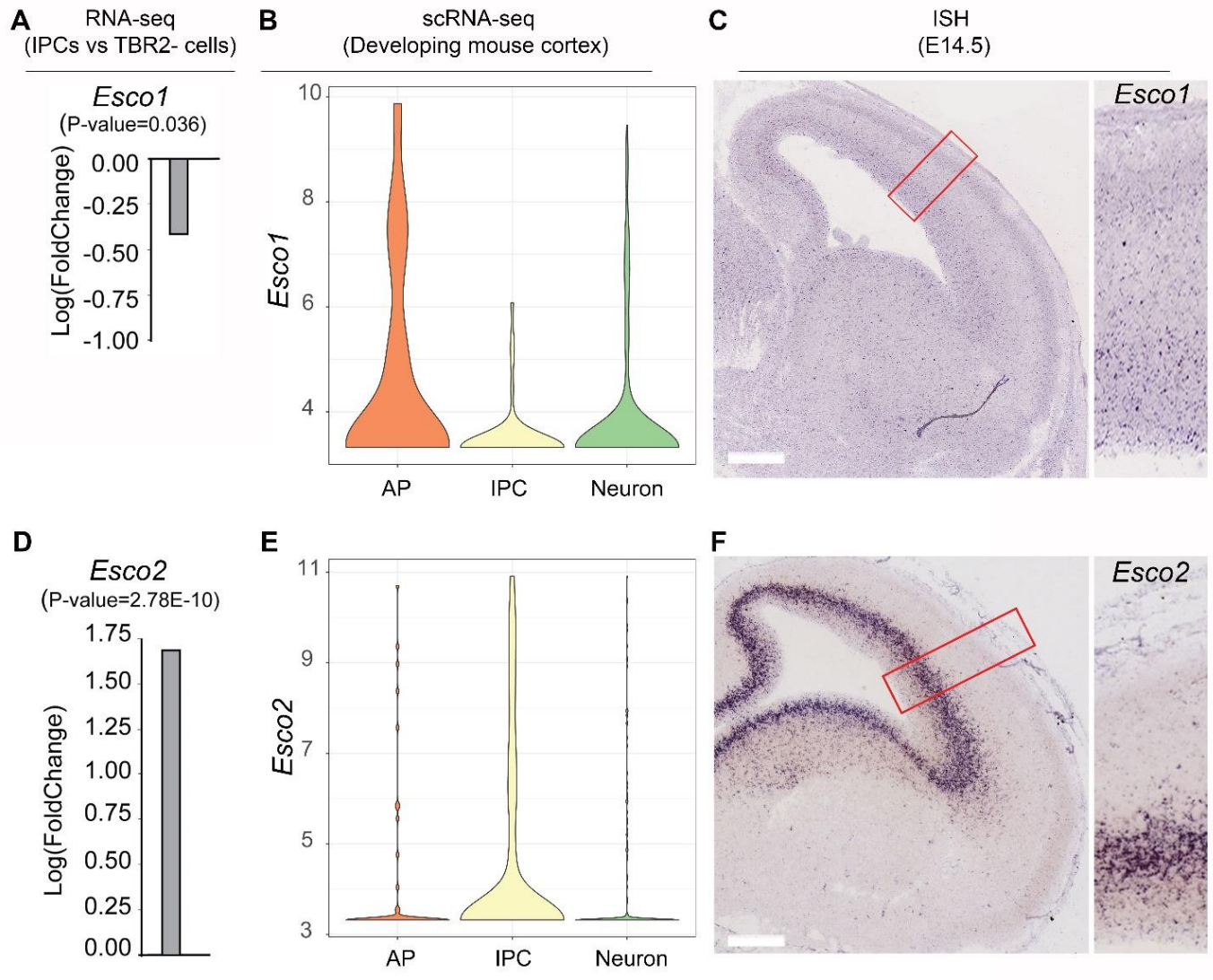
A
RNA-seq
(IPCs vs TBR2- cells)
Esco1
(P-value=0.036)
Log(FoldChange)
0.00
-0.25
-0.50
-0.75
-1.00
B
scRNA-seq
(Developing mouse cortex)
Esco1
10
8
6
4
AP
IPC
Neuron
C
ISH
(E14.5)
Esco1
D
Esco2
(P-value=2.78E-10)
Log(FoldChange)
1.75
1.50
1.25
1.00
0.75
0.50
0.25
0.00
E
Esco2
11
9
7
5
3
AP
IPC
Neuron
F
Esco2

Figure S5 (related to figure 6). Expression of ESCO1 and ESCO2 in the developing mouse cortex. (A–F) Expression of ESCO1 (A–C) and ESCO2 (D–F) were evaluated by RNA-seq with TBR2+ and TBR2- samples (A, D), single-cell (sc)RNA-seq (B, E), and ISH (C, F). (A, D) Bar graph indicating significant differential expression of ESCO1 (A) and ESCO2 (D) in TBR2+ IPCs compared with TBR2- cells in RNA-seq analysis. (B, E) Expression of *Esco1* (B) *Esco2* (E) based on a published single-cell scRNA-seq dataset of the developing mouse cortex (Telley et al., 2016). The graph-plots were generated using the Seurat package of R (Macosko et al., 2015) (http://genebrowser.unige.ch/science2016/). (C, F) Micrograph of *in situ* hybridization (ISH) staining showing prominence of *Esco1* (C) and *Esco2* (F) expression in VZ and SVZ of E14.5 mouse cortex, respectively. Magnified cortical region is shown with red box. Note that in contrast to a highly-enriched expression of *Esco1* in RGCs in VZ, expression of *Esco2* is mostly restricted in IPCs in SVZ. Abbreviations: RGC (Radial glial progenitor cell), IPC (Intermediate progenitor cell). Scale bar = 100 μm.

Figure S6

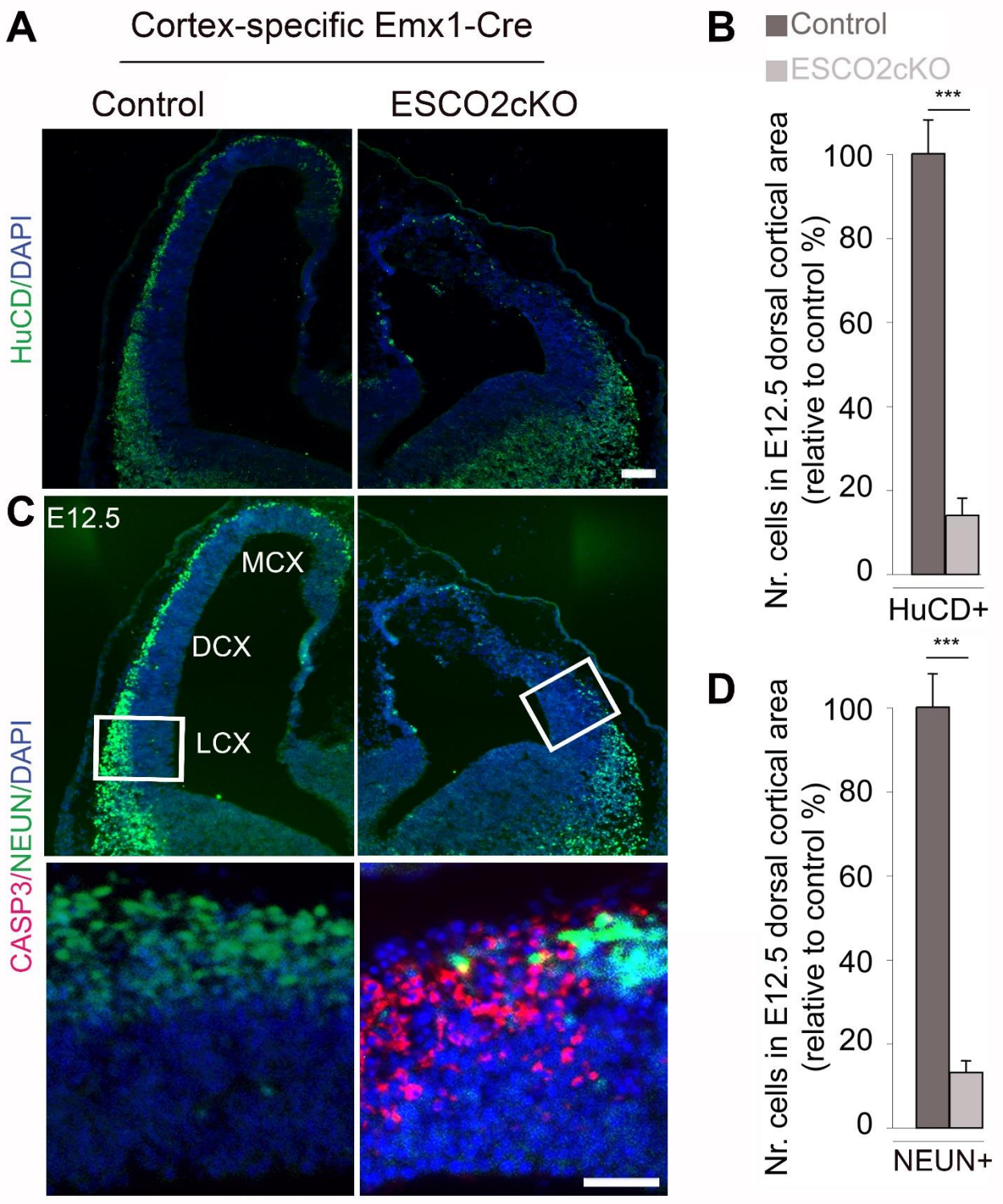
A
Cortex-specific Emx1-Cre
Control
ESCO2cKO
HuCD/DAPI
C
E12.5
MCX
DCX
LCX
CASP3/NEUN/DAPI
B
Control
ESCO2cKO
***
Nr. cells in E12.5 dorsal cortical area (relative to control %)
100
80
60
40
20
0
HuCD+
D
***
Nr. cells in E12.5 dorsal cortical area (relative to control %)
100
80
60
40
20
0
NEUN+

Figure S6 (related to figure 7). Deletion of ESCO2 in developing cortex causes depletion of post-mitotic neurons via apoptosis. (A, C) Immunohistochemical micrographs showing staining of the E12.5 mouse cortex with the antibodies HuCD and NeuN (pan-neuronal markers), and CASP3 to mark post-mitotic neurons undergoing apoptotic cell death. (B, D) Bar charts showing quantification of the number of HuCD+ and NeuN+ cells in the lateral aspect of the E12.5 cortex (marked with white box). The medial (MCX), dorsal (DCX), and lateral (LCX) cortical areas are indicated. *** *p*-value < 0.001, Experimental replicates (n) = 4 (B, D). Scale bar = 200 µm (A), 50 µm (C, lower panel).

- **Table S1 (related to figure 1).** Differential gene expression between TBR2+ IPCs and TBR2- cells (as a Supplemental Spreadsheet).
- **Table S2 (related to figure 1).** Selected gene ontology categories significantly enriched for TBR2+ IPC genes compared with TBR2- cell genes (as a supplemental spreadsheet).
- **Table S3 (related to figure 1).** List of validated IPC genes with their restricted expression in SVZ (as a Supplemental Spreadsheet).
- **Table S4 (related to figure 2).** List of cell cycle and chromosome segregation -related gene enriched in TBR2+ IPCs (as a Supplemental Spreadsheet).
- **Table S5 (related to figure 3).** List of apoptosis-related gene enriched in TBR2+ IPCs (as a Supplemental Spreadsheet).
- **Table S6 (related to figure 4).** List of TF-, chromatin remodeling-, epigenetic-, and lncRNA related genes enriched in TBR2+ IPCs (as a Supplemental Spreadsheet).
- **Table S7 (related to figure 5).** List of microcephaly-linked gene enriched in TBR2+ (as a Supplemental Spreadsheet).
- **Table S8 (related to figures 1, 6, 7, S2, S6)**. Statistical analyses (as a Supplemental Spreadsheet).

SUPPLEMENTAL EXPERIMENTAL PROCEDURES.

Plasmids

Plasmids used in this study: CAG-GFP-IRES-CRE (Zhao et al. 2006) from Addgene.

Antibodies

The following polyclonal (pAb) and monoclonal (mAb) primary antibodies used in this study were obtained from the indicated commercial sources: CASP3 rabbit pAb (1:100; Cell Signaling), ESCO2 (Whelan et al., 2012), GFP chick pAb (1:400; Abcam), HuCD mouse mAb (1:20; Invitrogen), NEUN mouse mAb (1:200, Chemicon), PAX6 mouse mAb (1:100; Developmental Studies Hybridoma Bank), PAX6 rabbit pAb (1:200; Covance), TBR2 rabbit pAb (1:200; Abcam), TBR2 rat 923 mAb (1:200; eBioscience).

Secondary antibodies used were Alexa 488-, Alexa 568-, Alexa 594- and Alexa 647-conjugated IgG (various species, 1:400; Molecular Probes).

Functional enrichment analysis of IPC genes

The lists of IPC genes (p-Value<0.01, log2FoldChange>1.0) were uploaded to the DAVID functional annotation tool (https://david.ncifcrf.gov/). Then, representative enriched biological functional terms were manually selected. To perform the Gene Set Enrichment Analysis (GSEA) analysis, the list of upregulated genes was uploaded to GSEA. Using FDR q-value<0.05 as a cut-off generated the enriched biological and cellular component terms. The Fisher's exact test was applied to identify the terms showing a statistically significant difference for the upregulated genes.

Identification of IPC-enriched lnRNAs

The lists of IPC genes (p-Value<0.01, log2FoldChange>1.0) were uploaded to the MGI gene nomenclature analysis tool (http://www.informatics.jax.org/batch). List of lnRNAs protein-encoding genes was extracted from each other.

Protein-Protein interaction network

The combined list of IPC-enrriched genes encoding for TFs (chromatin re modeling and epigenetic factors, Fig. 4J) was uploaded to the STRING database (http://string-db.org/). The protein-protein interactions from STRING were visualized by Cytoscape (https://cytoscape.org/; version: 3.3.0).

SUPPLEMENTAL DISCUSSION

Prominence of cell cycle-related factors in IPCs

Further unanswered questions that need to be addressed to increase our understanding of ICP cell biology include (1) the reasons behind shorter S-phase and longer G1-phase, and total length of cell cycle in IPCs than in RGCs, and (2) what factors drive the proliferation of some IPCs in cell cycle? In developing cortex, the length of G1 is increased in neurogenic progenitor cells compared with proliferative progenitors (Caviness et al., 2003; Dehay and Kennedy, 2007; Lukaszewicz et al., 2005; Salomoni and Calegari, 2010). As such, basal progenitors, including IPCs, are known to display a more extended G1 phase than RGCs (Calegari et al., 2005; Salomoni and Calegari, 2010). The increased G1 phase may support the more differentiative capacity of IPCs compared with RGCs, thus likely promoting IPC fate (Dehay and Kennedy, 2007; Lange et al., 2009). Indeed, functional manipulation of G1 length was shown to have effects that either support (i) IPC genesis leading to neurogenic division and premature neurogenesis (Calegari et al., 2005) or (ii) increased proliferative divisions, resulting in progenitor pool expansion, which manifests in cortical layer phenotypes later in development (Lange et al., 2009; Pilaz et al., 2009). Of note, we found a high expression of genes encoding for CDKs (*Cdk2*, *Cdk4*) with their regulator proteins (CCND1, CCND2, CCNE1, CCNE2), which drive the G1 phase of cycling IPCs. Hence, it is worth to examine the proliferation capacity of IPCs, in which the expression of these G1-phase factors is specifically manipulated.

Identification of new IPC-specific transcription factors

An intriguing molecular difference between the TBR2+ IPCs and the TBR2- cells in the developing mouse cortex is the differential expression of genes, which encode for different TF families (Table S5).

The zinc finger TFs form the largest protein family, having a wide range of molecular functions, and are involved in the development and differentiation of several cell lineages (Cassandri et al., 2017). Expression of many genes encoding for this TF family is enriched in IPCs. The role of the zinc finger proteins identified in this study in neurogenesis are largely unknown, except for that reported for the function of Uhrf1 in adult neurogenesis (Blanchart et al., 2018; Murao et al., 2019).

The second largest family of TFs is the bHLH TFs, which play key roles in various developmental processes in organisms from yeast to humans (Jones, 2004). Class I bHLH proteins are ubiquitously expressed, whereas class II bHLH proteins are tissue-specific. The nervous system-specific bHLH factors can further be classified into proneural and neural differentiation genes (Dennis et al., 2019). Two closely-related nescient helix loop helix 1 (*Nhlh1/bHLHa35*) and 2 (*Nhlh2/bHLHa34*) genes belong to the neural differentiation bHLH/Nscl subfamily genes (Dennis et al., 2019). In chicken, misexpression of *Nhlh1* leads to an abnormal brain structure with an underdeveloped cerebellum and a larger tectum caused by changes in cell proliferation (Li et al., 1999). *Nhlh1*-deficient mice exhibit a predisposition to arrhythmia leading to an early death due to autonomic nervous system dysfunction (Cogliati et al., 2002). The phenotype was more severe when *Nhlh1*-knockout mice were also heterozygous for *Nhlh2*. The specific and high expression of *Nhlh1* and *Nhlh2* in IPCs (Table. S5) suggests that the two factors act together to control the IPC differentiation. Expression of other bHLH TFs, including *Hes6/bHLHb41*, *Tcf3/bHLHb21*, *Tcf12/bHLHb20*, *Hey1/bHLHb31*, and *Ebf2*, *Srebf1/bHLHd1* were found to be enriched in IPCs. Among them, *Hes6*, *Tcf3*, *Tcf12*, *Hey1* and *Ebf2* were reported to be involved in neural development (Chuang et al., 2011; Gribble et al., 2009; Methot et al., 2013; Nam et al., 2016; Sakamoto et al., 2003; Uittenbogaard and Chiaramello, 2002; Yang et al., 2015). For *Srebf1*, no studies have yet been published on its role in neural development, albeit associations with Schizophrenia and Parkinson's disease have been reported, making a future investigation into its role in brain development even more interesting (Le Hellard et al., 2010; Lou et al., 2019; Yang et al., 2016).

The homeobox TFs were also found to be highly expressed in IPCs. Homeobox genes are important for the embryonic development of diverse animals, and are often comparatively analyzed to investigate evolution of animal development (Holland et al., 2007). Our investigation of genes enriched in IPC revealed three transcription factors that belong to the homeobox gene family. For two of the homeobox genes enriched in IPC, Meis homeobox 2 (*Meis2*) and POU domain, class 4, transcription factor 1 (*Pou4f1*, also called *Brn3a*), a role for neural development has already been described. MEIS2 has been described as a regulator of dorsal midbrain development interacting with the paired-box transcription factors PAX3 and PAX7 (Agoston et al., 2012). In humans, *MEIS2* mutations can cause intellectual disability (Douglas et al., 2018; Giliberti et al., 2019; Louw et al., 2015). In the developing nervous system, *Pou4f1* was shown to be essential for the generation of dorsal root ganglia sensory neurons and the regulation of sensory afferent projections (Zou et al., 2012). The other homeobox gene is the one cut domain family member 2 (*Onecut2*), which is well known as a master regulator in cancer (Lu et al., 2018; Rotinen et al., 2018). Function of ONECUT2 in brain development has not yet been described, however, *Onecut2* overexpression was shown to induce a neuron-like morphology and neuronal gene expression in fibroblasts making its role in neural development plausible (van der Raadt et al., 2019).

Another group of TF genes found to be enriched in IPC lineage is the myeloblastosis oncogene-like (Myb-like) transcription factor. The transcription factor MYBL1 (also called A-MYB) is known as a master regulator of meiosis (Bolcun-Filas et al., 2011), and in mice, it plays a vital role in spermatogenesis and mammary gland development (Toscani et al., 1997). Although *Mybl1* expression in neuronal progenitor cells has already been described (Trauth et al., 1994), its specific role in brain development is far from clear. Similarly, another Myb-like transcription factor, named MYBL2 or B-MYB was found to be enriched in IPC. MYBL2 is involved in cell proliferation and survival, however, these roles have been investigated mainly in cancer research and a possible function in neurogenesis has not been determined so far (Chen and Chen, 2018; Musa et al., 2017).

Altogether, our investigation of genes specific to IPCs revealed the expression of many transcription factors that were previously not known and, thus, are putative genetic

determinants of this cohort of neuronal progenitor cell type. Understanding the function of these IPC-enriched TFs would not only shed light on the mechanisms of cortical development, but also provide suggestions for ways to generate this cell type by direct reprograming from other cell linages.

Mutation of IPC-enriched genes is implicated in human neurodevelopmental disorders and neuropsychiatric diseases

The single-cell transcriptomic analysis of human developing cortex has identified a set of IPC genes (Fan et al., 2018; Li et al., 2018; Nowakowski et al., 2017; Pollen et al., 2015; Zhong et al., 2018). As part of further investigations, we compared in silico expression of such human IPC genes with our identified mouse IPC transcriptome to identify the developmental and evolutionary origin of the transcriptional signature of IPC cells. Our data suggest the existence of both conserved and non-conserved transcriptional signatures of IPCs in mammalian evolution. Consistent with this line of evidence, previous studies have shown that expression of TBR2 was found specifically in IPCs in lissencephalic rodent brain (Englund et al., 2005). In gyrencephalic ferret or primates, TBR2 labeled IPCs, and almost half of SOX2+, PAX6+ bRGC population (Betizeau et al., 2013; Fietz et al., 2010; Florio and Huttner, 2014; Hansen et al., 2010; Turrero Garcia et al., 2016). Furthermore, in rodent cortex, IPCs are predominately-neurogenic progenitors. However, in gyrencephalic species, IPCs are capable of self-amplification through symmetric proliferative divisions before their terminal division to generate neurons (Florio and Huttner, 2014; Lui et al., 2011). Beyond simply marking IPCs as transient progenitor cell type, future studies may have to relate and delve into the heterogeneity in the molecular milieu of IPCs in different species to afford elucidation of their contributions to cortical morphogenesis.

Advances in genetics and genomics studies in recent times have made it possible to identify many genetic coding and non-coding variants that cause neurodevelopmental disorders (D'Gama and Walsh, 2018; Hu et al., 2014; Juric-Sekhar and Hevner, 2019), with increased risk of neuropsychiatric disturbances (Sestan and State, 2018; Sullivan and Geschwind, 2019). Although we now have better insights into the genetic architecture

of neuropsychiatric perturbations, we still lack a comprehensive description of the underlying molecular and cellular mechanisms, mainly because of the heterogeneity of risk loci, and the involvement of multiple cell types and brain regions. Therefore, knowledge of the regulatory networks and the spatiotemporal distribution of these networks in the brain, is essential for elucidating which cell types are relevant in the etiology and possible treatment of these neurodevelopment- and neuropsychiatry-related disorders. Moreover, the clarification of the mechanistic underpinnings of any given neurological disorder also requires detailed understanding of the developmental events that are disrupted in the course of the disease, non-genic causatives (environmental or epigenetic) of the anomalies, and dissection of the eventual phenotype.

Gene co-expression analyses have also revealed that the developing human (Kang et al., 2011; Miller et al., 2014; Pletikos et al., 2014) or mouse (Loo et al., 2019) brain transcriptome can be organized into distinct co-expression networks with often prominent spatiotemporal patterns, and enriched for distinct biological functions. By probing the transcriptome of mouse IPCs and performing further analysis in the form of phenotype association categorization, we found strong connection between the identified IPC genes and known human neurodevelopmental disorders (Fig. 5). This can be explained by the essential role of IPCs in cortical development. A great proportion of cortical neurons can be traced to IPCs. IPC-derived neurons predominately form the upper cortical layers and their axons constitute the large interhemispheric commissural system (i.e., the corpus callosum). Cortical expansion and evolutionary changes have been attributed to the tremendous neurogenic output of TBR2-expressing IPCs and their diversity, especially in human. It is mainly for these reasons that disruption in the production of IPCs can lead to a wide range of cortical malformations and diverse neurological perturbations in the mammalian cortex. Our data thus suggest that disease-linked mutations of IPC genes might form robust groupings based on their GO profiles. These diseases clearly link to neurodevelopmental defects, e.g. cortical size-associated disorders (microcephaly, macrocephaly, and abnormal cortical gyration), corpus callosum defects (dysplastic, agenesis, aplasia, hypoplasia of corpus callosum, and abnormality of the cerebral white matter), and neurological deficits (intellectual disability, psychomotor developmental delay, schizophrenia, autism, and epilepsy).

Despite the recent great interest in elucidating the principles underlying the IPC-mediated evolutionary expansion of the neocortex and the consequence of related dysregulation, relatively less attention is accorded to dissecting disease-linked mutations of IPC genes to elucidate the pathophysiology of the attendant neurological disorder. By employing mouse model for the novel IPC gene *Esco2*, we were able to identify that IPCs may centrally rely on ESCO2 for survival and maintenance of their pool in the developing cortex. The absence of ESCO2, which is rather needed for the correct segregation of chromatids and therefore the genetic material into the progenies of dividing IPCs, may have triggered the massive apoptosis of the resultant ESCO2-deficient IPCs and the resultant overt cortical dysgenesis. Interestingly, *Esco2* mutations in human have been linked to neurological phenotypes, including microcephaly and cognitive deficits. The said pivotal role played by ESCO2 in IPC genesis and cortical morphogenesis recapitulated similar critical function of TBR2 in brain morphogenesis. Mutations that abolish *Tbr2* expression can cause severe neurodevelopmental abnormalities, including microcephaly, severe motor and cognitive delay, hypotonia, callosal agenesis, polymicrogyria, and cerebellar hypoplasia in rodent (Arnold et al., 2008; Sessa et al., 2008) and human (Baala et al. 2007). For future studies, linkage mapping and/or exome sequencing in human is expected to identify more IPC-related mutations and dysregulated genes associated with aberrant cortical architecture and growth.

To minimize gender bias in sampling for RNA-seq, we altogether used tissue from 15 embryos for 3 replicates. In addition, to examine the relative gender contribution in our samples, we compared the expression of chromosome X (*Xist*, *Pgk1*, *Hprt*, *Eif2s3x*) and chromosome Y (*Ddx3y*, *Eif2s3y*) - located genes, which are known housekeeping genes in the developing forebrain (Dewing et al. 2003; Cheung et al. 2017). The comparison revealed their comparable expression level in samples from TBR2+ IPCs and TBR2- cells (Fig. S1C). The data suggests that TBR2+ and TBR2- cell populations were derived from a similar number of female and male embryos. Nevertheless, the expression pattern of chromosome X/Y-located IPC genes should be validated by either IHC or ISH afore further investigation.

REFERENCES

Agoston, Z., Li, N., Haslinger, A., Wizenmann, A., and Schulte, D. (2012). Genetic and physical interaction of Meis2, Pax3 and Pax7 during dorsal midbrain development. BMC Dev Biol *12*, 10.
Arnold, S.J., Huang, G.J., Cheung, A.F., Era, T., Nishikawa, S., Bikoff, E.K., Molnar, Z., Robertson, E.J., and Groszer, M. (2008). The T-box transcription factor Eomes/Tbr2 regulates neurogenesis in the cortical subventricular zone. Genes Dev *22*, 2479-2484.
Betizeau, M., Cortay, V., Patti, D., Pfister, S., Gautier, E., Bellemin-Menard, A., Afanassieff, M., Huissoud, C., Douglas, R.J., Kennedy, H.*, et al.* (2013). Precursor diversity and complexity of lineage relationships in the outer subventricular zone of the primate. Neuron *80*, 442-457.
Blanchart, A., Navis, A.C., Assaife-Lopes, N., Usoskin, D., Aranda, S., Sontheimer, J., and Ernfors, P. (2018). UHRF1 Licensed Self-Renewal of Active Adult Neural Stem Cells. Stem Cells *36*, 1736-1751.
Bolcun-Filas, E., Bannister, L.A., Barash, A., Schimenti, K.J., Hartford, S.A., Eppig, J.J., Handel, M.A., Shen, L., and Schimenti, J.C. (2011). A-MYB (MYBL1) transcription factor is a master regulator of male meiosis. Development *138*, 3319-3330.
Calegari, F., Haubensak, W., Haffner, C., and Huttner, W.B. (2005). Selective lengthening of the cell cycle in the neurogenic subpopulation of neural progenitor cells during mouse brain development. J Neurosci 25, 6533-6538.
Cassandri, M., Smirnov, A., Novelli, F., Pitolli, C., Agostini, M., Malewicz, M., Melino, G., and Raschella, G. (2017). Zinc-finger proteins in health and disease. Cell Death Discov *3*, 17071.
Caviness, V.S., Jr., Goto, T., Tarui, T., Takahashi, T., Bhide, P.G., and Nowakowski, R.S. (2003). Cell output, cell cycle duration and neuronal specification: a model of integrated mechanisms of the neocortical proliferative process. Cereb Cortex 13, 592-598.
Chen, J., and Chen, X. (2018). MYBL2 Is Targeted by miR-143-3p and Regulates Breast Cancer Cell Proliferation and Apoptosis. Oncol Res *26*, 913-922.
Chuang, S.M., Wang, Y., Wang, Q., Liu, K.M., and Shen, Q. (2011). Ebf2 marks early cortical neurogenesis and regulates the generation of cajal-retzius neurons in the developing cerebral cortex. Dev Neurosci *33*, 479-493.
Cogliati, T., Good, D.J., Haigney, M., Delgado-Romero, P., Eckhaus, M.A., Koch, W.J., and Kirsch, I.R. (2002). Predisposition to arrhythmia and autonomic dysfunction in Nhlh1-deficient mice. Mol Cell Biol *22*, 4977-4983.
D'Gama, A.M., and Walsh, C.A. (2018). Somatic mosaicism and neurodevelopmental disease. Nat Neurosci *21*, 1504-1514.
Dehay, C., and Kennedy, H. (2007). Cell-cycle control and cortical development. Nat Rev Neurosci 8, 438-450.
Dennis, D.J., Han, S., and Schuurmans, C. (2019). bHLH transcription factors in neural development, disease, and reprogramming. Brain Res *1705*, 48-65.
Douglas, G., Cho, M.T., Telegrafi, A., Winter, S., Carmichael, J., Zackai, E.H., Deardorff, M.A., Harr, M., Williams, L., Psychogios, A.*, et al.* (2018). De novo missense variants in MEIS2 recapitulate the microdeletion phenotype of cardiac and palate abnormalities, developmental delay, intellectual disability and dysmorphic features. Am J Med Genet A *176*, 1845-1851.
Englund, C., Fink, A., Lau, C., Pham, D., Daza, R.A., Bulfone, A., Kowalczyk, T., and Hevner, R.F. (2005). Pax6, Tbr2, and Tbr1 are expressed sequentially by radial glia, intermediate progenitor cells, and postmitotic neurons in developing neocortex. J Neurosci *25*, 247-251.
Fan, X., Dong, J., Zhong, S., Wei, Y., Wu, Q., Yan, L., Yong, J., Sun, L., Wang, X., Zhao, Y.*, et al.* (2018). Spatial transcriptomic survey of human embryonic cerebral cortex by single-cell RNA-seq analysis. Cell research *28*, 730-745.

Fietz, S.A., Kelava, I., Vogt, J., Wilsch-Brauninger, M., Stenzel, D., Fish, J.L., Corbeil, D., Riehn, A., Distler, W., Nitsch, R.*, et al.* (2010). OSVZ progenitors of human and ferret neocortex are epithelial-like and expand by integrin signaling. Nat Neurosci *13*, 690-699.
Florio, M., and Huttner, W.B. (2014). Neural progenitors, neurogenesis and the evolution of the neocortex. Development *141*, 2182-2194.
Giliberti, A., Curro, A., Papa, F.T., Frullanti, E., Ariani, F., Coriolani, G., Grosso, S., Renieri, A., and Mari, F. (2019). MEIS2 gene is responsible for intellectual disability, cardiac defects and a distinct facial phenotype. Eur J Med Genet.
Gribble, S.L., Kim, H.S., Bonner, J., Wang, X., and Dorsky, R.I. (2009). Tcf3 inhibits spinal cord neurogenesis by regulating sox4a expression. Development *136*, 781-789.
Hansen, D.V., Lui, J.H., Parker, P.R., and Kriegstein, A.R. (2010). Neurogenic radial glia in the outer subventricular zone of human neocortex. Nature *464*, 554-561.
Holland, P.W., Booth, H.A., and Bruford, E.A. (2007). Classification and nomenclature of all human homeobox genes. BMC Biol *5*, 47.
Hu, W.F., Chahrour, M.H., and Walsh, C.A. (2014). The diverse genetic landscape of neurodevelopmental disorders. Annual review of genomics and human genetics *15*, 195-213.
Jones, S. (2004). An overview of the basic helix-loop-helix proteins. Genome Biol *5*, 226.
Juric-Sekhar, G., and Hevner, R.F. (2019). Malformations of Cerebral Cortex Development: Molecules and Mechanisms. Annu Rev Pathol *14*, 293-318.
Kang, H.J., Kawasawa, Y.I., Cheng, F., Zhu, Y., Xu, X., Li, M., Sousa, A.M., Pletikos, M., Meyer, K.A., Sedmak, G.*, et al.* (2011). Spatio-temporal transcriptome of the human brain. Nature *478*, 483-489.
Kawaguchi, A., Ikawa, T., Kasukawa, T., Ueda, H.R., Kurimoto, K., Saitou, M., and Matsuzaki, F. (2008). Single-cell gene profiling defines differential progenitor subclasses in mammalian neurogenesis. Development *135*, 3113-3124.
Lange, C., Huttner, W.B., and Calegari, F. (2009). Cdk4/cyclinD1 overexpression in neural stem cells shortens G1, delays neurogenesis, and promotes the generation and expansion of basal progenitors. Cell Stem Cell 5, 320-331.
Le Hellard, S., Muhleisen, T.W., Djurovic, S., Ferno, J., Ouriaghi, Z., Mattheisen, M., Vasilescu, C., Raeder, M.B., Hansen, T., Strohmaier, J.*, et al.* (2010). Polymorphisms in SREBF1 and SREBF2, two antipsychotic-activated transcription factors controlling cellular lipogenesis, are associated with schizophrenia in German and Scandinavian samples. Mol Psychiatry *15*, 463-472.
Li, C.M., Yan, R.T., and Wang, S.Z. (1999). Misexpression of a bHLH gene, cNSCL1, results in abnormal brain development. Dev Dyn *215*, 238-247.
Li, M., Santpere, G., Imamura Kawasawa, Y., Evgrafov, O.V., Gulden, F.O., Pochareddy, S., Sunkin, S.M., Li, Z., Shin, Y., Zhu, Y.*, et al.* (2018). Integrative functional genomic analysis of human brain development and neuropsychiatric risks. Science *362*.
Li, Z., Tyler, W.A., Zeldich, E., Santpere Baro, G., Okamoto, M., Gao, T., Li, M., Sestan, N., and Haydar, T.F. (2020). Transcriptional priming as a conserved mechanism of lineage diversification in the developing mouse and human neocortex. Science advances *6*.
Loo, L., Simon, J.M., Xing, L., McCoy, E.S., Niehaus, J.K., Guo, J., Anton, E.S., and Zylka, M.J. (2019). Single-cell transcriptomic analysis of mouse neocortical development. Nat Commun *10*, 134.
Lou, F., Li, M., Liu, N., Li, X., Ren, Y., and Luo, X. (2019). The polymorphism of SREBF1 gene rs11868035 G/A is associated with susceptibility to Parkinson's disease in a Chinese population. Int J Neurosci *129*, 660-665.

Louw, J.J., Corveleyn, A., Jia, Y., Hens, G., Gewillig, M., and Devriendt, K. (2015). MEIS2 involvement in cardiac development, cleft palate, and intellectual disability. Am J Med Genet A *167A*, 1142-1146.
Lu, T., Wu, B., Yu, Y., Zhu, W., Zhang, S., Zhang, Y., Guo, J., and Deng, N. (2018). Blockade of ONECUT2 expression in ovarian cancer inhibited tumor cell proliferation, migration, invasion and angiogenesis. Cancer Sci *109*, 2221-2234.
Lui, J.H., Hansen, D.V., and Kriegstein, A.R. (2011). Development and evolution of the human neocortex. Cell *146*, 18-36.
Lukaszewicz, A., Savatier, P., Cortay, V., Giroud, P., Huissoud, C., Berland, M., Kennedy, H., and Dehay, C. (2005). G1 phase regulation, area-specific cell cycle control, and cytoarchitectonics in the primate cortex. Neuron 47, 353-364.
Macosko, E.Z., Basu, A., Satija, R., Nemesh, J., Shekhar, K., Goldman, M., Tirosh, I., Bialas, A.R., Kamitaki, N., Martersteck, E.M.*, et al.* (2015). Highly Parallel Genome-wide Expression Profiling of Individual Cells Using Nanoliter Droplets. Cell *161*, 1202-1214.
Methot, L., Hermann, R., Tang, Y., Lo, R., Al-Jehani, H., Jhas, S., Svoboda, D., Slack, R.S., Barker, P.A., and Stifani, S. (2013). Interaction and antagonistic roles of NF-kappaB and Hes6 in the regulation of cortical neurogenesis. Mol Cell Biol *33*, 2797-2808.
Miller, J.A., Ding, S.L., Sunkin, S.M., Smith, K.A., Ng, L., Szafer, A., Ebbert, A., Riley, Z.L., Royall, J.J., Aiona, K.*, et al.* (2014). Transcriptional landscape of the prenatal human brain. Nature *508*, 199-206.
Murao, N., Matsubara, S., Matsuda, T., Noguchi, H., Mutoh, T., Mutoh, M., Koseki, H., Namihira, M., and Nakashima, K. (2019). Np95/Uhrf1 regulates tumor suppressor gene expression of neural stem/precursor cells, contributing to neurogenesis in the adult mouse brain. Neurosci Res *143*, 31-43.
Musa, J., Aynaud, M.M., Mirabeau, O., Delattre, O., and Grunewald, T.G. (2017). MYBL2 (B-Myb): a central regulator of cell proliferation, cell survival and differentiation involved in tumorigenesis. Cell Death Dis *8*, e2895.
Nam, S.M., Kim, Y.N., Kim, J.W., Kyeong, D.S., Lee, S.H., Son, Y., Shin, J.H., Kim, J., Yi, S.S., Yoon, Y.S.*, et al.* (2016). Hairy and Enhancer of Split 6 (Hes6) Deficiency in Mouse Impairs Neuroblast Differentiation in Dentate Gyrus Without Affecting Cell Proliferation and Integration into Mature Neurons. Cell Mol Neurobiol *36*, 57-67.
Nowakowski, T.J., Bhaduri, A., Pollen, A.A., Alvarado, B., Mostajo-Radji, M.A., Di Lullo, E., Haeussler, M., Sandoval-Espinosa, C., Liu, S.J., Velmeshev, D.*, et al.* (2017). Spatiotemporal gene expression trajectories reveal developmental hierarchies of the human cortex. Science *358*, 1318-1323.
Pilaz, L.J., Patti, D., Marcy, G., Ollier, E., Pfister, S., Douglas, R.J., Betizeau, M., Gautier, E., Cortay, V., Doerflinger, N., et al. (2009). Forced G1-phase reduction alters mode of division, neuron number, and laminar phenotype in the cerebral cortex. Proc Natl Acad Sci U S A 106, 21924-21929.
Pletikos, M., Sousa, A.M., Sedmak, G., Meyer, K.A., Zhu, Y., Cheng, F., Li, M., Kawasawa, Y.I., and Sestan, N. (2014). Temporal specification and bilaterality of human neocortical topographic gene expression. Neuron *81*, 321-332.
Pollen, A.A., Nowakowski, T.J., Chen, J., Retallack, H., Sandoval-Espinosa, C., Nicholas, C.R., Shuga, J., Liu, S.J., Oldham, M.C., Diaz, A.*, et al.* (2015). Molecular identity of human outer radial glia during cortical development. Cell *163*, 55-67.

Rotinen, M., You, S., Yang, J., Coetzee, S.G., Reis-Sobreiro, M., Huang, W.C., Huang, F., Pan, X., Yanez, A., Hazelett, D.J.*, et al.* (2018). ONECUT2 is a targetable master regulator of lethal prostate cancer that suppresses the androgen axis. Nat Med *24*, 1887-1898.
Sakamoto, M., Hirata, H., Ohtsuka, T., Bessho, Y., and Kageyama, R. (2003). The basic helix-loop-helix genes Hesr1/Hey1 and Hesr2/Hey2 regulate maintenance of neural precursor cells in the brain. J Biol Chem *278*, 44808-44815.
Salomoni, P., and Calegari, F. (2010). Cell cycle control of mammalian neural stem cells: putting a speed limit on G1. Trends Cell Biol 20, 233-243.
Sessa, A., Mao, C.A., Hadjantonakis, A.K., Klein, W.H., and Broccoli, V. (2008). Tbr2 directs conversion of radial glia into basal precursors and guides neuronal amplification by indirect neurogenesis in the developing neocortex. Neuron *60*, 56-69.
Sestan, N., and State, M.W. (2018). Lost in Translation: Traversing the Complex Path from Genomics to Therapeutics in Autism Spectrum Disorder. Neuron *100*, 406-423.
Sullivan, P.F., and Geschwind, D.H. (2019). Defining the Genetic, Genomic, Cellular, and Diagnostic Architectures of Psychiatric Disorders. Cell *177*, 162-183.
Telley, L., Govindan, S., Prados, J., Stevant, I., Nef, S., Dermitzakis, E., Dayer, A., and Jabaudon, D. (2016). Sequential transcriptional waves direct the differentiation of newborn neurons in the mouse neocortex. Science *351*, 1443-1446.
Toscani, A., Mettus, R.V., Coupland, R., Simpkins, H., Litvin, J., Orth, J., Hatton, K.S., and Reddy, E.P. (1997). Arrest of spermatogenesis and defective breast development in mice lacking A-myb. Nature *386*, 713-717.
Trauth, K., Mutschler, B., Jenkins, N.A., Gilbert, D.J., Copeland, N.G., and Klempnauer, K.H. (1994). Mouse A-myb encodes a trans-activator and is expressed in mitotically active cells of the developing central nervous system, adult testis and B lymphocytes. EMBO J *13*, 5994-6005.
Turrero Garcia, M., Chang, Y., Arai, Y., and Huttner, W.B. (2016). S-phase duration is the main target of cell cycle regulation in neural progenitors of developing ferret neocortex. J Comp Neurol *524*, 456-470.
Uittenbogaard, M., and Chiaramello, A. (2002). Expression of the bHLH transcription factor Tcf12 (ME1) gene is linked to the expansion of precursor cell populations during neurogenesis. Brain Res Gene Expr Patterns *1*, 115-121.
van der Raadt, J., van Gestel, S.H.C., Nadif Kasri, N., and Albers, C.A. (2019). ONECUT transcription factors induce neuronal characteristics and remodel chromatin accessibility. Nucleic Acids Res *47*, 5587-5602.
Whelan, G., Kreidl, E., Wutz, G., Egner, A., Peters, J.M., and Eichele, G. (2012). Cohesin acetyltransferase Esco2 is a cell viability factor and is required for cohesion in pericentric heterochromatin. EMBO J *31*, 71-82.
Yang, L., Chen, J., Li, Y., Wang, Y., Liang, S., Shi, Y., Shi, S., and Xu, Y. (2016). Association between SCAP and SREBF1 gene polymorphisms and metabolic syndrome in schizophrenia patients treated with atypical antipsychotics. World J Biol Psychiatry *17*, 467-474.
Yang, Q., Liu, S., Yin, M., Yin, Y., Zhou, G., and Zhou, J. (2015). Ebf2 is required for development of dopamine neurons in the midbrain periaqueductal gray matter of mouse. Dev Neurobiol *75*, 1282-1294.
Zhong, S., Zhang, S., Fan, X., Wu, Q., Yan, L., Dong, J., Zhang, H., Li, L., Sun, L., Pan, N.*, et al.* (2018). A single-cell RNA-seq survey of the developmental landscape of the human prefrontal cortex. Nature *555*, 524-528.
Zou, M., Li, S., Klein, W.H., and Xiang, M. (2012). Brn3a/Pou4f1 regulates dorsal root ganglion sensory neuron specification and axonal projection into the spinal cord. Dev Biol *364*, 114-127.